


# Quantum Interface for Noble-Gas Spins Based on Spin-Exchange Collisions

Or Katz<sup>1,2</sup>, Roy Shaham,<sup>1,2</sup> and Ofer Firstenberg<sup>1,\*</sup>

<sup>1</sup>*Department of Physics of Complex Systems, Weizmann Institute of Science, 76100 Rehovot, Israel*

<sup>2</sup>*Rafael Ltd., 31021 Haifa, Israel*

 (Received 7 May 2019; accepted 15 November 2021; published 10 January 2022)

An ensemble of noble-gas nuclear spins is a unique quantum system that could maintain coherence for many hours at room temperature and above, owing to exceptional isolation from the environment. This isolation, however, is a mixed blessing, limiting the ability of these ensembles to interface with other quantum systems coherently. Here we show that spin-exchange collisions with alkali-metal atoms render a quantum interface for noble-gas spins without impeding their long coherence times. We formulate the many-body theory of the hybrid system and reveal a collective mechanism that strongly couples the macroscopic quantum states of the two spin ensembles. Despite their stochastic and random nature, weak collisions enable entanglement and reversible exchange of nonclassical excitations in an efficient, controllable, and deterministic process. With recent experiments now entering the strong-coupling regime, this interface paves the way toward realizing hour-long quantum memories and entanglement at room temperature.

DOI: [10.1103/PRXQuantum.3.010305](https://doi.org/10.1103/PRXQuantum.3.010305)

## I. INTRODUCTION

Macroscopic systems exhibiting quantum behavior at or above room temperature are of great scientific interest. One such prominent system is a hot vapor of alkali-metal atoms enclosed in a vacuum cell. The collective spin state of these ensembles, consisting of as many as  $10^{14}$  atoms, has been used to demonstrate quantum spin squeezing, storage and control of single-excitation quanta, and entanglement at room temperature [1–18]. Despite the rapid thermal motion and atomic collisions, the coherence time of the collective spin in these studies reaches milliseconds and beyond. In some settings, it is unaffected by frequent spin-exchange collisions [18–20] and is essentially limited by the electron spins' coupling to their surroundings.

Odd isotopes of noble gases, such as  $^3\text{He}$ , possess a nonzero nuclear spin. This spin is optically inaccessible and well protected from the external environment by the enclosing, full, electronic shells and is therefore extremely long-lived. Noble-gas spin ensembles have demonstrated lifetimes  $T_1$  exceeding hundreds of hours and coherence times  $T_2^*$  of 100 h at or above room temperature [21–24]. It is to be expected that the collective nuclear spin in these

ensembles, similarly to the collective electronic spin in alkali vapor, can be brought to the quantum limit and utilized for quantum optics and sensing applications. Several studies have proposed the use of collisions with optically excited metastable  $^3\text{He}$  atoms to generate and read out nonclassical states of ground-level  $^3\text{He}$  spins, relying on collisional exchange of electronic configurations that leads to adiabatic transfer of the quantum state [25–28].

Here we study a different mechanism forming a quantum interface with noble-gas spins. The mechanism relies on the stochastic accumulation of weak spin-exchange collisions, directly coupling between the collective spins of polarized atomic gases and thus not limited to adiabatic transfer rates. Recently, we experimentally demonstrated the coherent coupling between alkali-vapor spins and noble-gas spins in the regime where the coherent exchange rate dominates the spin rotation rate [29]. Additionally, we have demonstrated a bidirectional interface between light and noble-gas spins, using the optically accessible alkali spins as mediators [30]. These experiments establish the coherent nature of the collective coupling for classical (coherent) states. If the coupling is indeed quantum (i.e., if it transfers nonclassical correlations between the spin ensembles), then it can be used for quantum information applications, such as quantum memories and remote entanglement with long-lived noble-gas spins [31–33].

Here we provide a theoretical description of the emergent collective coupling between the spins of polarized alkali and noble-gas atoms. We analyze the effect of weak spin-exchange collisions using a many-body formalism

\*ofer.firstenberg@weizmann.ac.il

Published by the American Physical Society under the terms of the [Creative Commons Attribution 4.0 International](https://creativecommons.org/licenses/by/4.0/) license. Further distribution of this work must maintain attribution to the author(s) and the published article's title, journal citation, and DOI.

and find that they can efficiently couple the collective quantum excitations of the two ensembles, with negligible quantum noise added due to the collisions' stochasticity. We derive the strong-coupling conditions, where the quantum-coherent exchange dominates over the relaxation. We use numerical many-body simulations and a detailed analytical model to study the controllable periodic exchange of nonclassical states between the spin ensembles, further attesting to the quantum nature of the interface, and discuss potential applications. Finally, we outline practical experimental conditions for the efficient exchange of nonclassical states between the alkali and noble-gas ensembles.

This paper is organized as follows. In Sec. II we describe the system under study and review the mean-field model, which is commonly used to describe its semiclassical dynamics. In Sec. III we present numerical stochastic simulations that demonstrate quantum dynamics of a few spin excitations between the collective spin states studied in this work. In Sec. IV we present a detailed many-body model and derive the equations of motion for the collective states of the spin gases. In Sec. V we discuss different coupling regimes of the two spin gases. In Sec. VI we demonstrate the formalism for the exchange of nonclassical states and discuss their potential application for quantum metrology. In Sec. VII we numerically solve the equations of motion of the detailed model and demonstrate quantum exchange of states for a feasible experimental configuration. Finally, in Sec. VIII we conclude and discuss the role of imperfect polarization on the results.

## II. SYSTEM AND MEAN-FIELD MODEL

Noble-gas spins can be accessed via spin-exchange collisions with alkali-vapor atoms. Consider a gaseous mixture of  $N_B$  noble-gas atoms with nuclear spin  $1/2$  and  $N_A \ll N_B$  alkali-metal atoms, all enclosed in a heated spherical cell of volume  $V$  and undergoing frequent collisions. A collision between noble-gas atom  $b$  and alkali atom  $a$  is governed by the Fermi-contact interaction and described by the evolution operator  $\exp(-i\phi\hat{\mathbf{k}}_b \cdot \hat{\mathbf{s}}_a)$ , where  $\hat{\mathbf{k}}_b$  is the noble-gas nuclear spin operator,  $\hat{\mathbf{s}}_a$  is the alkali electronic spin operator of the colliding atoms labeled  $a$  and  $b$ , respectively, and  $\phi$  is the mutual precession angle; see Figs. 1(a) and 1(b) [34–36]. While  $\phi$  varies between collisions depending on the atoms' random trajectories, its value is always positive [37,38]. This is an important property of the isotropic Fermi-contact interaction, leading to a nonzero mean precession  $\langle\phi\rangle$  during collisions.

Between collisions, the electron and nuclear spins of the *alkali* atoms are altered by their strong hyperfine coupling. Consequently, the slow dynamics of alkali atoms having nuclear spin  $I > 0$  is determined by the operator sum  $\hat{\mathbf{f}}_a = \hat{\mathbf{s}}_a + \hat{\mathbf{i}}_a$ , where  $\hat{\mathbf{i}}_a$  is the nuclear spin operator of alkali atom  $a$ . We focus on the conditions of high alkali atomic density

and small Zeeman splitting. Under these conditions, the alkali Zeeman states are populated with a spin-temperature distribution, and  $\hat{\mathbf{f}}_a = q\hat{\mathbf{s}}_a$ , where  $q$  is the Larmor slowing-down factor [ $2I + 1 < q < 4I^2/3 + 4I/3 + 1$  depending on the degree of polarization; see Eq. (18)] [35,39].

The accepted formalism for describing the dynamics of the spin ensembles uses the mean-field Bloch equations [11]:

$$\begin{aligned}\partial_t\langle\hat{\mathbf{f}}\rangle &= n_B\zeta\langle\hat{\mathbf{k}}\rangle \times \langle\hat{\mathbf{f}}\rangle + n_Bk_{\text{SE}}q\langle\hat{\mathbf{k}}\rangle - \gamma_A\langle\hat{\mathbf{f}}\rangle, \\ \partial_t\langle\hat{\mathbf{k}}\rangle &= n_A\zeta\langle\hat{\mathbf{f}}\rangle \times \langle\hat{\mathbf{k}}\rangle + n_Ak_{\text{SE}}\langle\hat{\mathbf{f}}\rangle/q - \gamma_B\langle\hat{\mathbf{k}}\rangle.\end{aligned}\quad (1)$$

Here  $n_A = N_A/V$  and  $n_B = N_B/V$  are the atomic densities,  $\zeta = \langle\sigma v\phi\rangle/q$  denotes the mean-field interaction strength, where  $\sigma$  is the spin-exchange cross section and  $v$  is the relative thermal velocity, and  $k_{\text{SE}} \equiv (1/4)\langle v\sigma\phi^2\rangle$  is the binary spin-exchange rate coefficient [11]. The first term in the expressions in Eq. (1) describes the mutual average precession of the two mean spins. The second term represents an incoherent transfer of spin polarization from one species to another (conserving the total spin) [35]; it is commonly used to initially polarize the noble-gas spins via so-called spin-exchange optical pumping (SEOP) [34]. The alkali-metal spins are strongly coupled to the environment, leading to spin rotation at rate

$$\gamma_A = n_B(k_{\text{SE}} + \sigma_{\text{SR}}v) + n_A\sigma_{\text{SD}}v_A/2, \quad (2)$$

consisting of the spin-exchange interaction with the noble-gas nuclei, collisional spin-rotation coupling (cross section  $\sigma_{\text{SR}}$  and thermally averaged reduced velocity  $v$ ), and spin destruction via binary collisions of alkali-metal spins (cross section  $\sigma_{\text{SD}}$  and mean atomic velocity  $v_A$ ) [11]. The relaxation rate of the noble-gas spins is given by

$$\gamma_B = k_{\text{SE}}n_A + T_B^{-1}, \quad (3)$$

where  $T_B$  is the coherence time in the absence of alkali atoms, usually limited by inhomogeneity of the magnetic field [23,34]. Typically,  $\gamma_B \ll \gamma_A$ , where for hybrid systems in a centimeter-sized cell,  $\gamma_B$  is a fraction of  $1 \text{ h}^{-1}$  and  $\gamma_A$  is in the range from 10 to  $1000 \text{ s}^{-1}$ .

The mean-field equations, Eq. (1), implicitly assume that any quantum correlation developed between different atoms due to collisions is rapidly lost. Therefore, this model is insufficient for describing the dynamics of nonclassical (i.e., quantum) spin states.

## III. SIMPLIFIED MANY-BODY MODEL

### A. Collective spin states

We describe the macroscopic quantum states of the spin ensembles using collective spin operators [2]. Each col-

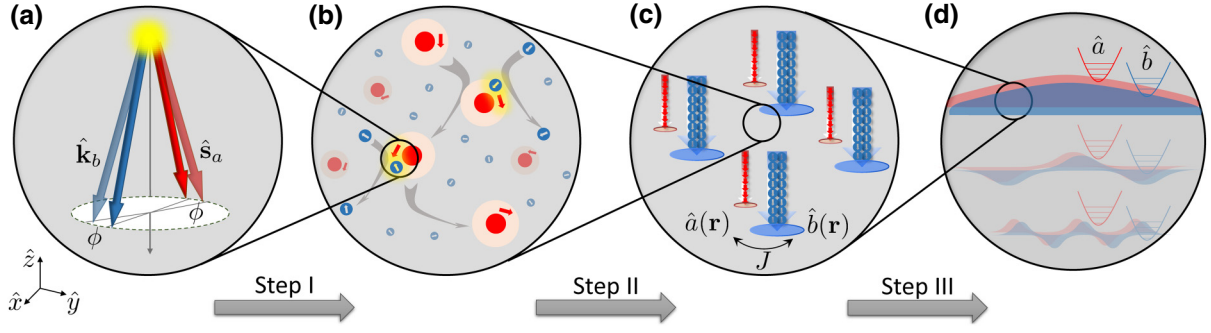


FIG. 1. Quantum interface for noble-gas spins via spin-exchange collisions. (a) Coherent interaction during a collision between alkali-metal electronic spin  $\hat{s}_a$  (red) and noble-gas nuclear spin  $\hat{k}_b$  (blue). The two spins mutually precess and acquire an angle  $\phi \ll 1$  while conserving the total spin, where  $\phi$  is random and depends on the collision kinematics. (b) Stochastic sequence of collisions. Spin exchange occurs over a few picoseconds when the valence electron's wave function (pink) overlaps with the noble-gas nucleus (blue). (c) For polarized ensembles, multiple collisions between different atoms accumulate to a coherent dynamics of bosonic collective-spin excitations, described by local quantum operators  $\hat{a}(\mathbf{r})$  (alkali) and  $\hat{b}(\mathbf{r})$  (noble gas) and a coupling rate  $J$ . Incoherent spin dynamics, which enables initialization via spin-exchange optical pumping, play a minor role for  $\phi \ll 1$ . (d) Diffusion of the gas atoms and the boundary conditions in the cell define nonlocal spin modes. The lowest-order spatial modes  $\hat{a}$  and  $\hat{b}$  govern the coherent evolution of the collective quantum spins (see Sec. IV D and Ref. [40]).

lective operator is a symmetric superposition of the spins in the cell, where  $\hat{\mathbf{F}} = \sum_{a=1}^{N_A} \hat{\mathbf{f}}_a$  is the collective alkali spin operator and  $\hat{\mathbf{K}} = \sum_{b=1}^{N_B} \hat{\mathbf{k}}_b$  is the collective noble-gas spin operator. Here we focus on the particular regime of highly polarized ensembles, with most of the spins pointing downwards ( $-\hat{z}$ ) [1–3]. In this regime, the operators  $\hat{F}_z$  and  $\hat{K}_z$  can be approximated by their classical expectation values  $F_z = -p_A N_A q/2$  and  $K_z = -p_B N_B/2$ , where  $p_A, p_B \leq 1$  are the degrees of spin polarization ( $p_A = p_B = 1$  for the ideal preparation of fully polarized ensembles). The quantum state of the collective spins is then fully captured by the ladder operators  $\hat{F}^\pm = \hat{F}_x \pm i\hat{F}_y$  and  $\hat{K}^\pm = \hat{K}_x \pm i\hat{K}_y$ . Pictorially, for polarized ensembles, these operators describe a small tilt of the macroscopic spin vector, accompanied by spin uncertainty that scales as  $\sqrt{N_A}$  for the alkali ensemble and  $\sqrt{N_B}$  for the noble gas.

To see how quantum spin excitations are associated with these operators, we apply the Holstein-Primakoff transformation [2], which describes the collective states in terms of excitations of bosonic fields. We define the annihilation operators of the two ensembles as  $\hat{a} = \hat{F}^- / \sqrt{2|F_z|}$  and  $\hat{b} = \hat{K}^- / \sqrt{2|K_z|}$ . The state  $|0\rangle_A |0\rangle_B$ , with zero spins pointing upwards, is identified as the vacuum, and the creation operators  $\hat{a}^\dagger$  and  $\hat{b}^\dagger$  flip upwards one alkali or noble-gas spin. For the special case of coherent spin states, the dynamics is captured in the mean-field model [Eq. (1)] by use of the transformations  $\langle \hat{a} \rangle = \sqrt{N_A/q p_A} \langle \hat{f}^- \rangle$  and  $\langle \hat{b} \rangle = \sqrt{N_B/p_B} \langle \hat{k}^- \rangle$ , which associate the collective displacements with the mean spin of the ensembles. In what follows, we discuss quantum states that can be represented by these operators, whose dynamics cannot be described by the mean-field model.

## B. Stochastic simulation

To examine the quantum nature of the alkali–noble-gas interaction, we first develop a simplified stochastic many-body simulation. The simulation tracks the quantum state of many spins that randomly collide. It computes their Hamiltonian dynamics in the absence of external sources of relaxation, by formally setting  $\gamma_A$  and  $\gamma_B$  to zero in Eqs. (2) and (3). For simplicity, the simulation assumes that  $I = 0$  (i.e.,  $\hat{\mathbf{f}}_a \equiv \hat{\mathbf{s}}_a$ ), that all spins are nearly polarized, and that all spins are equally likely to collide with each other. We alleviate these assumptions and consider additional relaxation mechanisms in Sec. IV.

In each simulation time step, we pair each electron spin with a single random noble-gas spin and describe their evolution due to collision. The duration of each time step corresponds to the mean time between collisions of an alkali atom with any of the noble-gas atoms  $\tau = 1/(n_B \sigma v)$ . The collision between spins  $a$  and  $b$  at time step  $n$  is described by the exchange Hamiltonian

$$\mathcal{V}_{ab}^{(n)} = \frac{\phi_a^{(n)}}{\tau} (\hat{s}_{az} \hat{k}_{bz} + \frac{1}{2} \hat{s}_a^+ \hat{k}_b^- + \frac{1}{2} \hat{k}_b^+ \hat{s}_a^-), \quad (4)$$

where  $\hat{s}_a^+, \hat{s}_a^-, \hat{k}_b^+$  and  $\hat{k}_b^-$  are ladder spin operators. The collision angle  $\phi_a^{(n)}$  is a random variable, sampled from a Gaussian distribution  $\mathcal{N}(\langle \phi \rangle, \delta \phi)$  with mean  $\langle \phi \rangle$  and typical standard deviation  $\delta \phi = \langle \phi \rangle$ , where  $\langle \phi \rangle \ll 1$  is an input parameter.

The simulation also includes the response of the alkali spins to an axial magnetic field via the Hamiltonian term  $g_A B_z \sum_a \hat{s}_{az}$ , where  $g_A$  is the gyromagnetic ratio of the

alkali spins. As discussed in Sec. V, we choose the particular magnetic field  $g_A B_z \tau = \langle \phi \rangle / 2$  in which the precession of the two gases is synchronized ( $\omega_A = \omega_B$ ), thus maximizing the coupling between the two spin gases.

The scattering matrix per electron spin  $a$  at time step  $n$  is then given by

$$U_n^{(a)} = \sum_b \chi_{ab}^{(n)} e^{i\frac{1}{2}\phi_a^{(n)}} \left[ i \sin\left(\frac{1}{2}\phi_a^{(n)}\right) (|\downarrow\uparrow\rangle\langle\uparrow\downarrow| + |\uparrow\downarrow\rangle\langle\downarrow\uparrow|) - 2 \sin^2\left(\frac{1}{4}\phi_a^{(n)}\right) (|\uparrow\downarrow\rangle\langle\uparrow\downarrow| + |\downarrow\uparrow\rangle\langle\downarrow\uparrow|) \right] + \mathbb{1}, \quad (5)$$

where  $|\downarrow\uparrow\rangle \equiv |\downarrow_a\rangle_A |\uparrow_b\rangle_B$ ,  $|\uparrow\downarrow\rangle \equiv |\uparrow_a\rangle_A |\downarrow_b\rangle_B$ , and  $\mathbb{1}$  is the identity operator. The pair selection is encapsulated in the random variable  $\chi_{ab}^{(n)}$ , with  $\chi_{ab}^{(n)} = 1$  if spins  $a$  and  $b$  collide and  $\chi_{ab}^{(n)} = 0$  otherwise. We constrain the pairing process by  $\chi_{ab}^{(n)} \chi_{cb}^{(n)} = 0$  for  $a \neq c$ , ensuring that each noble-gas spin interacts at most with a single electron spin at each time step. Finally, the wave function of the system evolves as

$$|\psi(n+1)\rangle = \Pi_a U_n^{(a)} |\psi(n)\rangle. \quad (6)$$

We numerically use two different Hilbert subspaces in which nearly all spins point downwards. One subspace describes a single spin-up excitation, represented by the wave functions

$$|\psi(t)\rangle = \sum_{i=1}^{N_A+N_B} c_i(t) |\downarrow \dots \downarrow \uparrow_i \downarrow \dots \downarrow\rangle_{a\&b}$$

for a set of complex-valued coefficients  $c_i(t)$  satisfying  $\sum_i |c_i(t)|^2 = 1$ . We use this subspace to simulate  $N_A = 100$  and  $N_B = 10^4$  atoms. The second subspace, comprising two spin excitations, is represented by the wave functions

$$|\psi(t)\rangle = \sum_{i \neq j}^{N_A+N_B} c_{ij}(t) |\downarrow \dots \downarrow \uparrow_i \downarrow \dots \downarrow \uparrow_j \downarrow \dots \downarrow\rangle_{a\&b}$$

for  $\sum_{i \neq j} |c_{ij}(t)|^2 = 1$ , and we use it with  $N_A = 30$  and  $N_B = 300$ . Importantly, absent external relaxations, the single-excitation and double-excitation subspaces are invariant to the exchange operation due to conservation of the total spin. This enables simulation of a relatively large number of atoms at moderate subspace dimensions.

### C. Numerical results

The exchange dynamics for a single spin excitation are shown in Fig. 2. We initialize the system with either the symmetric excitation  $|\psi_0\rangle = |1\rangle_A |0\rangle_B \equiv N_A^{-1/2} \sum_a \hat{f}_a^+ |0\rangle_A |0\rangle_B$  [Figs. 2(a) and 2(c)] or a localized

excitation  $|\psi_0\rangle = |\uparrow\downarrow \dots \downarrow\rangle_A |0\rangle_B$  [Figs. 2(b) and 2(d)]. The exchange between the two ensembles emerges as a collective phenomenon: for the symmetric Fock state, we observe multiple, high-contrast oscillations of the populations of the collective states, whereas for the localized excitation, the oscillations are negligible and scale with the small overlap  $\langle 1 | \uparrow\downarrow \dots \downarrow \rangle_A = 1/\sqrt{N_A}$ . The transfer amplitude accumulates constructively only for the excitation that is symmetrically shared among all spins, maximizing the periodic exchange rate and fidelity. The rate of the collective oscillations is given by  $2J = \sqrt{N_A/N_B} \langle \phi \rangle / \tau$ . The comparison between the evolution of the different initial states emphasizes the collective nature of the coupling, which is taken for granted in the mean-field description.

Importantly, the dominance of the coherent exchange over the incoherent transfer and dephasing relies on the collisions being very weak. To exemplify this, we compare  $\langle \phi \rangle = 2 \times 10^{-2}$  [Figs. 2(a) and 2(b)] and  $\langle \phi \rangle = 10^{-5}$  [Figs. 2(c) and 2(d)], the latter corresponding to realistic  $^3\text{He-K}$  collisions. For  $\langle \phi \rangle = 2 \times 10^{-2}$ , we observe a dephasing and thermalization of the alkali spin with the noble-gas spins at rate  $\gamma_A = \alpha \langle \phi^2 \rangle / 4\tau$ , with  $\alpha \leq 1$ , reducing the exchange fidelity compared with that with  $\langle \phi \rangle = 10^{-5}$ . For fully polarized noble-gas spins  $\alpha = 1/2$  when  $\delta\phi \ll \langle \phi \rangle$  and the randomness of the collision process results solely from randomness in pairing of colliding atoms. When  $\delta\phi \gg \langle \phi \rangle$ ,  $\alpha = 1$  due to additional randomness in collision intensity, making collisions less correlated. The observed decay rate fully agrees with the mean-field relaxation rate of the alkali spins,  $n_B k_{\text{SE}}$ . Note also that the noble-gas spin dephasing  $\gamma_B = (N_A/N_B) \gamma_A$  is negligible since  $N_A \ll N_B$ . We have verified that the exchange and decoherence depend only weakly on the chosen parameters and distributions.

Finally, we simulate the periodic bunching of two spin excitations with  $\langle \phi \rangle = 10^{-5}$  and  $|\psi_0\rangle = |1\rangle_A |1\rangle_B$ , as shown in Fig. 2(e). This evolution is analogous to the nonclassical Hong-Ou-Mandel phenomenon with a beam splitter with variable reflectivity. At  $t = \pi m / 2J$  for any integer  $m$ , the two excitations are bunched in either of the two spin ensembles (analogous to the ports of the beam splitter), generating an entangled state.

These simulations demonstrate that the collisional interface supports the reversible, high-fidelity, full exchange of nonclassical states between the two spin ensembles despite the stochastic nature of the spin-exchange interaction in the gas.

### D. The exchange mechanism

To elucidate the physical mechanism that renders a deterministic exchange out of random collisions, we analytically describe the quintessential case of the exchange

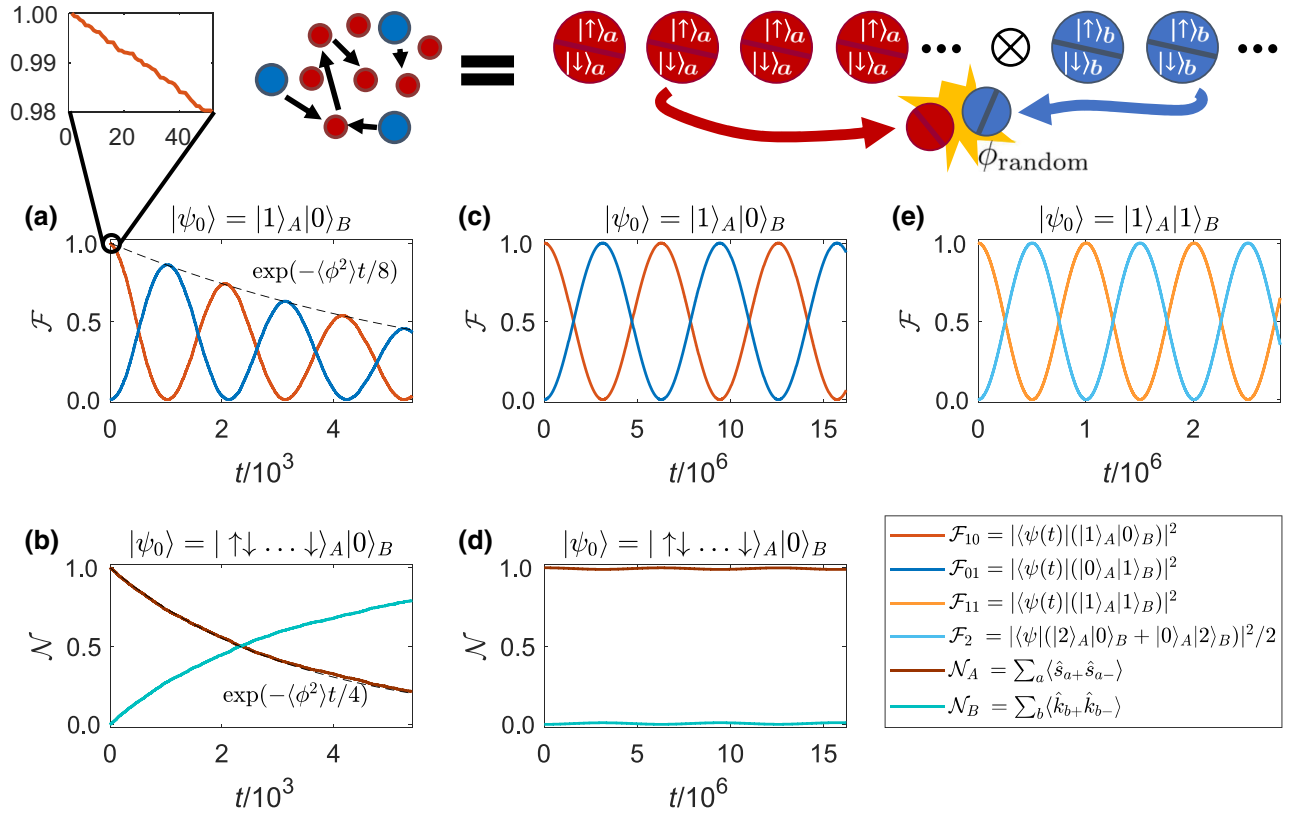


FIG. 2. Stochastic simulation of the collisional interface. We solve the unitary evolution of the quantum state of  $N_A = 100$  electron spins and  $N_B = 10^4$  noble-gas spins [in (e),  $N_A = 30$  and  $N_B = 300$ ], initialized in the state  $|\psi_0\rangle$ . Each electron spin undergoes a spin-exchange collision of random strength ( $\phi_{\text{random}} \ll 1$ ) with a randomly chosen noble-gas spin every simulation time step  $\tau = 1$ ; The collisions are either very weak,  $\langle\phi\rangle = 10^{-5}$  (c)–(e), or more moderate,  $\langle\phi\rangle = 2 \times 10^{-2}$  (a),(b). The electron spins can be initialized with all pointing downwards  $|0\rangle_A = |\downarrow \dots \downarrow\rangle_A$  (“vacuum”), or with one arbitrary spin pointing upwards  $\hat{f}_{a=1}^+ |0\rangle_A = |\uparrow \downarrow \dots \downarrow\rangle_A$  (“localized excitation”) or in the symmetric state with a single collective excitation  $|1\rangle_A = N_A^{-1/2} \sum_a \hat{f}_a^+ |0\rangle_A = N_A^{-1/2} \sum_i |\downarrow \dots \uparrow_i \downarrow \dots \downarrow\rangle_A$  (“collective excitation”). The nuclear spins are initialized in either  $|0\rangle_B$  or  $|1\rangle_B$ . (a) An initial symmetric excitation  $|\psi_0\rangle = |1\rangle_A |0\rangle_B$  is coherently exchanged between the two spin ensembles. The inset highlights the stochasticity of the process. The exchange is accompanied by dephasing due to incoherent transfer of the excitation to the large noble-gas ensemble ( $N_B \gg N_A$ ) via the same process underlying SEOP. (b) The localized excitation is incoherently transferred to the noble gas. (c) Strikingly, when the collisions are weaker, the exchange fidelities  $\mathcal{F}_{10}$  and  $\mathcal{F}_{01}$  oscillate with higher contrast and nearly no decay, despite the stochasticity of the process. (d) Almost no oscillations are observed for the localized excitation. (e) When  $|\psi_0\rangle = |1\rangle_A |1\rangle_B$ , the two excitations periodically “bunch” in a superposition of either of the spin ensembles ( $|2\rangle_A |0\rangle_B + |0\rangle_A |2\rangle_B$ ), manifesting the nonclassical Hong-Ou-Mandel phenomenon and validating the quantum beam-splitter property of the interface.

of a single spin excitation. The noble-gas spins are initialized in the state  $|0\rangle_B$  with all spins pointing down, and the alkali spins are initialized in the nonclassical Fock state  $|1\rangle_A \equiv N_A^{-1/2} \sum_a \hat{f}_a^+ |0\rangle_A$  (i.e., a symmetric superposition with one of the spins pointing up). After a short time  $t$ , the system wavefunction  $|1\rangle_A |0\rangle_B$  evolves by Eq. (6) into

$$|1\rangle_A |0\rangle_B - iJt|0\rangle_A |1\rangle_B - i\epsilon|\delta\psi\rangle + \mathcal{O}(\langle\phi^2\rangle). \quad (7)$$

This evolution, with  $Jt, \epsilon \ll 1$ , is the onset of transfer of the single spin excitation from the alkali to the noble gas via both deterministic and stochastic contributions; the Fock state  $|1\rangle_B \equiv N_B^{-1/2} \sum_b \hat{k}_b^+ |0\rangle_B$  manifests the deterministic transfer. The stochastic amplitude  $\epsilon$  and the

stochastic wave function  $|\delta\psi\rangle$ , which represents an incoherent mixture of excited spins, are given in Eqs. (A1) and (A2) in Appendix A.

To quantify the corresponding transition amplitudes  $Jt$  and  $\epsilon$ , we average the stochastic amplitude under the assumption that every alkali atom is equally likely to collide with any noble-gas atom at mean time between collisions  $\tau$ . We then find that

$$Jt = \frac{1}{2}(\langle\phi\rangle t/\tau) \sqrt{N_A/N_B} \quad (8)$$

and that, after many collisions, the stochastic variable  $\epsilon$  follows the central limit theorem

$$\epsilon \rightarrow \sqrt{\langle\phi^2\rangle t/2\tau}. \quad (9)$$

These results show that, at longer times, the transition amplitude of the deterministic term in Eq. (7) dominates the transition amplitude of the stochastic term, resulting in  $Jt \gg \epsilon$ . It is therefore the accumulated mean effect of many weak collisions that leads to deterministic transfer scaling linearly with  $t/\tau$ , while fluctuations add up at a reduced rate  $\sqrt{t/\tau}$  due to their incoherent nature.

#### IV. DETAILED MODEL OF THE MANY-BODY PROBLEM

##### A. Derivation outline

We now derive an extended analytical model describing the quantum dynamics of the collective spins of the two gases and accounting for several relaxation mechanisms, finite nuclear spin of the alkali, and spatial diffusion of the gases. The derivation steps are illustrated in Fig. 1 and correspond to the different scales of the problem. The first step (Sec. B) provides the coherent scattering of alkali and noble-gas pairs by short binary collisions. We focus on the limit of weak collisions ( $\langle \phi \rangle \ll 1$ ), in which the collective dynamics appear coherent. The second step (Sec. C) yields the coarse-grained spin-exchange interaction between local collective spins. Here we find that symmetrically oriented spins of the ensemble within a unit volume interact coherently, whereas the stochasticity of collisions generates coupling to other, nonsymmetric spin states. The latter manifests itself as relaxation and introduces quantum noise, which remarkably follows vacuum statistics and therefore has minimal variance. The last step (Sec. D) introduces other decay processes and spatial diffusion in the gas. We consider the spatial modes of the collective spin that host macroscopic nonclassical correlations and identify the uniform spin mode of the noble gas as the least-decaying mode. We then derive the equations of motion describing the coupling between the collective modes of the alkali and noble-gas spins. The results of this model are discussed in Sec. V and are demonstrated for several nonclassical states in Sec. VI.

##### B. Step I: Spin-exchange interaction

The Hamiltonian of the two spin ensembles we consider is given by  $\mathcal{H}(t) = \mathcal{H}_0 + \mathcal{V}(t)$ , where

$$\mathcal{H}_0 = \hbar a_{\text{hpf}} \sum_a \hat{\mathbf{i}}_a \hat{\mathbf{s}}_a + \hbar \tilde{\omega}_A q \sum_a \hat{s}_{a,z} + \hbar \tilde{\omega}_B \sum_b \hat{k}_{b,z} \quad (10)$$

is the noninteracting Hamiltonian of the two spin ensembles, where  $a_{\text{hpf}}$  denotes the hyperfine coupling constant in the ground state of the alkali atom [11] and  $\tilde{\omega}_A$  and  $\tilde{\omega}_B$  are the Larmor frequencies of the alkali and noble-gas spins induced by an external magnetic field  $\mathbf{B} = B\hat{z}$ . The microscopic many-body interaction Hamiltonian, governed by

the Fermi-contact interaction [36,37], is given by

$$\mathcal{V}(t) = \sum_{a=1}^{N_A} \sum_{b=1}^{N_B} \hbar \alpha_{ab}(t) \hat{\mathbf{s}}_a \cdot \hat{\mathbf{k}}_b. \quad (11)$$

This form conserves the total spin of the colliding pairs. The instantaneous interaction strength  $\alpha_{ab}(t)$  between atoms  $a$  and  $b$  is determined by the specific microscopic trajectory of each atom.

We model the spatial degrees of freedom of the thermal atoms as classical. Their coordinates  $\mathbf{r}_a(t)$  and  $\mathbf{r}_b(t)$  follow ballistic trajectories, which are independent of the spin state and are governed by the classical Langevin equation. The collisions in the gas can be considered as sudden and binary; the mean collision duration  $\tau_c$  is only a few picoseconds [11], whereas the mean time between collisions for an alkali atom  $\tau$  is a few nanoseconds at ambient pressure. Since collisions are isolated in time ( $\tau_c \ll \tau$ ), the interaction strength can be approximated by a train of instantaneous events  $\alpha_{ab}(t) = \sum_i \hbar \phi_{ab}^{(i)} \delta(t - t_{ab}^{(i)})$ , where  $\phi_{ab}^{(i)}$  denotes the phase  $\phi$  that spins  $a$  and  $b$  accumulate during the  $i$ th collision and  $t_{ab}^{(i)}$  denotes the time of the collision, as determined from the particle trajectories derived in Appendix B [see Eq. (B3)].

We consider short times  $\tau'$ , typically a few tens of picoseconds, such that  $\tau \gg \tau' \gg \tau_c$ , for which each atom experiences at most a single collision. In other words, we assume that if a collision occurred between an alkali spin  $a$  and a noble-gas spin  $b$ , then neither  $a$  nor  $b$  collided with other atoms during  $\tau'$ . Consequently,  $\mathcal{V}(t)$  in Eq. (11) has no more than one appearance of each spin operator and thus commutes with itself. Under these conditions, the time-evolution operator is simplified to

$$U_I(t + \tau', t) = \exp\left(-i \sum_{ab} \sum_i^{t'} \phi_{ab}^{(i)} \hat{\mathbf{s}}_a \cdot \hat{\mathbf{k}}_b\right), \quad (12)$$

where  $\sum_i^{t'}$  denotes the sum over all collision instances that occur during the short time interval in which  $t_{ab}^{(i)} \in [t, t + \tau']$ . For weak collisions, the mutual precession is small  $\phi_{ab}^{(i)} \ll 1$ , and the exponential term in Eq. (12) can be expanded to leading orders in  $\phi$  as a Dyson series:

$$U_I \approx U_I^{(0)} + U_I^{(1)} + U_I^{(2)} + \dots \quad (13)$$

Here the lowest-order terms are  $U_I^{(0)}(t + \tau', t) = \mathbb{1}$  (the identity),

$$U_I^{(1)}(t + \tau', t) = -i \sum_{ab} \sum_i^{t'} \phi_{ab}^{(i)} \hat{\mathbf{s}}_a \cdot \hat{\mathbf{k}}_b,$$

and

$$U_I^{(2)}(t + \tau', t) = -\frac{1}{2} \sum_{abcd} \sum_{ij}^{\tau'} \phi_{ab}^{(i)} \phi_{cd}^{(j)} (\hat{\mathbf{s}}_a \cdot \hat{\mathbf{k}}_b) (\hat{\mathbf{s}}_c \cdot \hat{\mathbf{k}}_d).$$

This simplified form provides for the evolution of any quantum mechanical operator  $\hat{A}$  after time  $\tau'$ ,  $\Delta\hat{A} = U^\dagger(t + \tau', t) \hat{A}(t) U(t + \tau', t) - \hat{A}(t)$ , where  $U = e^{-i\mathcal{H}_0\tau'} U_I$  is in the Heisenberg picture. Note that  $e^{-i\mathcal{H}_0\tau'}$  and  $U_I$  commute, as explained below. Up to second order in  $\phi$ , the dynamics of  $\hat{A}$  is given by

$$\frac{1}{\tau'} \Delta\hat{A} = -\frac{i}{\hbar} [\hat{A}, \mathcal{H}_0] - \frac{i}{\hbar} [\hat{A}, \mathcal{V}] + \mathcal{L}(\hat{A}). \quad (14)$$

The first term is the standard Hamiltonian evolution governed by  $\mathcal{H}_0$  and independent of  $\phi$ . The second term describes a unitary evolution during a collision with an effective Hamiltonian

$$\mathcal{V} = \sum_{ab} \sum_i^{\tau'} \frac{\hbar}{\tau'} \phi_{ab}^{(i)} \hat{\mathbf{s}}_a \cdot \hat{\mathbf{k}}_b, \quad (15)$$

which is first order in  $\phi$ . The third term,  $\mathcal{L}(A)$ , is proportional to  $\phi^2$  and has the structure of a standard Lindblad term:

$$\mathcal{L}(A) = -\frac{1}{2} \sum_{ab} \sum_i^{\tau'} (\phi_{ab}^{(i)})^2 \left[ \hat{\mathbf{s}}_a \cdot \hat{\mathbf{k}}_b, [\hat{\mathbf{s}}_a \cdot \hat{\mathbf{k}}_b, \hat{A}] \right]. \quad (16)$$

We note, however, that this operator is not associated with a decay but is rather a second-order correction to the unitary evolution.

The evolution of the single-spin operators  $\hat{\mathbf{s}}_a$  and  $\hat{\mathbf{k}}_b$  in the time interval  $\tau'$  are then derived from Eq. (14), yielding

$$\begin{aligned} \Delta\hat{\mathbf{s}}_a &= \sum_n \sum_i^{\tau'} \phi_{an}^{(i)} [\hat{\mathbf{k}}_n \times \hat{\mathbf{s}}_a + \phi_{an}^{(i)} (\hat{\mathbf{k}}_n - \hat{\mathbf{s}}_a)/4], \\ \Delta\hat{\mathbf{k}}_b &= \sum_m \sum_i^{\tau'} \phi_{mb}^{(i)} [\hat{\mathbf{s}}_m \times \hat{\mathbf{k}}_b + \phi_{mb}^{(i)} (\hat{\mathbf{s}}_m - \hat{\mathbf{k}}_b)/4]. \end{aligned} \quad (17)$$

This form conserves the total spin of each colliding pair  $a$ - $b$ , since  $\Delta(\hat{\mathbf{s}}_a + \hat{\mathbf{k}}_b) = 0$ . Equation (17) describes the mutual precession of pairs of spins, as illustrated in Fig. 1(a). This evolution is unitary to second order in the precession angle  $\phi$ , while high-order contributions are neglected in the truncation of Eq. (13).

At longer times ( $ta_{\text{hpf}} \gg 1$ ), the nuclear spin of the *alkali* atoms is altered by the strong hyperfine interaction with the electron, such that slow dynamics are described in terms of  $\hat{\mathbf{f}}_a$ . From now on, we focus on alkali ensembles in a spin-temperature population distribution, for which

$\hat{\mathbf{f}}_a = q\hat{\mathbf{s}}_a$ , with the slowing-down factor  $q = q(I, p_A)$  given by [41]

$$q(I, p_A) = \frac{2I + 1}{p_A} \frac{(1 + p_A)^{2I+1} + (1 - p_A)^{2I+1}}{(1 + p_A)^{2I+1} - (1 - p_A)^{2I+1}} - \frac{1}{p_A^2} + 1. \quad (18)$$

### C. Step II: Local collective interaction

The slow evolution of the spins depends on the cumulative effect of multiple collisions among different atoms. At the macroscopic limit, it is formidable to keep track of the kinematic details of all atoms, given a large set of collision times  $t_{ab}^{(i)}$  and strengths  $\phi_{ab}^{(i)}$ . Instead, we represent the exact values of  $t_{ab}^{(i)}$  and  $\phi_{ab}^{(i)}$  by their equivalent random variables:

$$\begin{aligned} \sum_i^{\tau'} \phi_{ab}^{(i)} &\rightarrow \varkappa_{ab}(t, \tau') \phi_a(t), \\ \sum_i^{\tau'} (\phi_{ab}^{(i)})^2 &\rightarrow \varkappa_{ab}(t, \tau') \phi_a^2(t), \end{aligned} \quad (19)$$

where  $\varkappa_{ab}(t, \tau')$  is a Bernoulli process indicating whether a collision between particles  $a$  and  $b$  has occurred during the short time interval  $[t, t + \tau']$ , with  $\tau' \gg \hbar/a_{\text{hpf}}$ . As the phase  $\phi_a$  depends on the kinematic parameters of the collision, such as the impact parameter and the two-body reduced velocity [34], we treat it as a random variable, with mean  $\langle \phi \rangle$  and variance  $\text{var} \phi$ . The operation  $\langle \cdot \rangle$  denotes an average over the microscopic kinematic parameters. The stochastic nature of  $\phi_a$  models the randomness in the interaction strength, while the stochastic nature of  $\varkappa_{ab}$  models the randomness in pairing the colliding atoms.

We derive the statistical properties of  $\varkappa_{ab}$  as a function of the microscopic kinematic variables in Appendix B in a small control volume, yielding

$$\begin{aligned} \langle \varkappa_{ab}(t, \tau') \rangle &= v\sigma\tau'w(\mathbf{r}_a - \mathbf{r}_b), \\ \langle \varkappa_{ab}(t, \tau') \varkappa_{cd}(t', \tau') \rangle &= \delta_{ac}\delta_{bd}\tau'\delta(t - t') \langle \varkappa_{ab}(t, \tau') \rangle. \end{aligned} \quad (20)$$

Here the window function  $w(\mathbf{r}) = \Theta(l - |\mathbf{r}|)/V_l$  represents a control volume  $V_l = 4\pi l^3/3$ , where  $\Theta$  is the Heaviside function and  $l$  is the coarse-graining scale (larger than the atoms' mean free path).

We are now set to perform spatial coarse graining. First, we replace the discrete atomic operators with the continuous operators  $\hat{\mathbf{f}}(\mathbf{r}, t) \equiv \sum_a \hat{\mathbf{f}}_a(t) \delta[\mathbf{r} - \mathbf{r}_a(t)]$  and  $\hat{\mathbf{k}}(\mathbf{r}, t) \equiv \sum_b \hat{\mathbf{k}}_b(t) \delta[\mathbf{r} - \mathbf{r}_b(t)]$  (see Refs. [2,5]). We then perform the spatial convolutions  $\hat{\mathbf{f}}(\mathbf{r}, t) \rightarrow \hat{\mathbf{f}}(\mathbf{r}, t) * w(\mathbf{r})$  and  $\hat{\mathbf{k}}(\mathbf{r}, t) \rightarrow \hat{\mathbf{k}}(\mathbf{r}, t) * w(\mathbf{r})$ . Importantly, after coarse graining the spin operators  $\hat{\mathbf{f}}(\mathbf{r}, t)$  and  $\hat{\mathbf{k}}(\mathbf{r}, t)$  become *local symmetric* operators and the spatial coordinate  $\mathbf{r}$  supersedes the specific particle labels. The use of these symmetric spin operators is motivated by the results in Sec. III; for sufficiently weak collisions, we expect that the coherent coupling between  $\hat{\mathbf{f}}(\mathbf{r}, t)$  and  $\hat{\mathbf{k}}(\mathbf{r}, t)$  will be enhanced over

the sum of incoherent couplings to other, nonsymmetric spin operators. We therefore assume that the coarse-graining volume  $V_l$  contains a large number of particles  $V_l n_A, V_l n_B \gg 1$  for the central-limit theorem and the enhancement of the coupling of symmetric modes to hold.

Using Eqs. (17), (19), and (20), we now describe the collisional part of the evolution of  $\hat{\mathbf{f}}(\mathbf{r}, t)$  and  $\hat{\mathbf{k}}(\mathbf{r}, t)$  at time intervals much longer than  $\tau'$  by

$$\begin{aligned}\partial_t \hat{\mathbf{f}} &= \zeta \hat{\mathbf{k}} \times \hat{\mathbf{f}} - k_{\text{SE}n_B} \hat{\mathbf{f}} + q k_{\text{SE}n_A} \hat{\mathbf{k}} + \hat{\mathbf{F}}_{\text{ex}}, \\ \partial_t \hat{\mathbf{k}} &= \zeta \hat{\mathbf{f}} \times \hat{\mathbf{k}} - k_{\text{SE}n_A} \hat{\mathbf{k}} + \frac{1}{q} k_{\text{SE}n_B} \hat{\mathbf{f}} - \hat{\mathbf{F}}_{\text{ex}}.\end{aligned}\quad (21)$$

The first term in the expressions in Eq. (21) represents the average mutual precession of the two symmetric spin operators within the coarse-graining volume, with the local interaction strength given by  $\zeta \equiv \langle \sigma v \phi \rangle / q$ . As it describes coherent dynamics, it can be associated with an effective spin-exchange Hamiltonian

$$\mathcal{V}_{\text{ex}} = \hbar \zeta \int d^3 \mathbf{r}_A \int d^3 \mathbf{r}_B \delta(\mathbf{r}_A - \mathbf{r}_B) \hat{\mathbf{f}}(\mathbf{r}_A, t) \cdot \hat{\mathbf{k}}(\mathbf{r}_B, t).\quad (22)$$

The second and third terms in the expressions in Eq. (21) represent incoherent transfer of spin polarization from one species to the other, while conserving the total spin. Recall that we assume a spin-1/2 noble gas. Here  $n_A = \sum_a w(\mathbf{r} - \mathbf{r}_a)$  and  $n_B = \sum_b w(\mathbf{r} - \mathbf{r}_b)$  denote the local densities of the two spin ensembles, and  $k_{\text{SE}} \equiv (1/4) \langle v \sigma \phi^2 \rangle$  corresponds to the binary spin-exchange rate coefficient [11] presented in Eq. (1). In particular, the term  $k_{\text{SE}n_B} \hat{\mathbf{f}}/q$  is responsible for hyperpolarization of the noble gas by optically pumped alkali-metal spins, underlying the SEOP technique [11,34]. The incoherent SEOP term here replaces the coherent  $\mathcal{L}(A)$  defined in Eq. (16); it has the same functional form but is now essentially incoherent due to the coarse graining of the microscopic kinematics. Notably, incoherent effects are second order in  $\phi$ , and since  $\langle \phi^2 \rangle / \langle \phi \rangle \ll 1$  (typically  $10^{-5}$ ),  $\zeta$  is substantially larger than  $k_{\text{SE}}$ . For example, the precession angle for a  $\text{K}^3\text{He}$  collision is  $\langle \phi \rangle \approx \zeta q / \sigma v = 1.4 \times 10^{-5}$  rad, and  $\langle \phi^2 \rangle \approx 4 k_{\text{SE}} / \sigma v = 1.6 \times 10^{-10}$  rad<sup>2</sup> (see Appendix D).

The fluctuation vector operator  $\hat{\mathbf{F}}_{\text{ex}}(\mathbf{r})$  in Eq. (21) encompasses the coupling of the operators  $\hat{\mathbf{f}}(\mathbf{r})$  and  $\hat{\mathbf{k}}(\mathbf{r})$  to all other nonsymmetric combinations of spins residing within that coarse-grained unit volume at  $\mathbf{r}$ . In Appendix C, we derive the statistical properties of  $\hat{\mathbf{F}}_{\text{ex}}$  for this system and show that it acts as a quantum noise process and that, for polarized states, it has vacuum statistics [42]. Notably, the expressions in Eq. (21) are consistent with the mean-field model when taking expectation values and considering classical properties, as we demonstrate in Appendix D.

### D. Step III: Dynamics with diffusion and relaxation

To describe the spatial dynamics of a macroscopic ensemble of alkali and noble-gas spins in the presence of relaxation, we add terms to the expressions in Eq. (21) and write the Heisenberg-Langevin equations for  $\hat{\mathbf{f}}(\mathbf{r}, t)$  and  $\hat{\mathbf{k}}(\mathbf{r}, t)$ :

$$\begin{aligned}\partial_t \hat{\mathbf{f}} &= -\frac{i}{\hbar} [\hat{\mathbf{f}}, \mathcal{H}_l + \mathcal{V}_{\text{ex}}] + D_A \nabla^2 \hat{\mathbf{f}} - \gamma_A \hat{\mathbf{f}} + \hat{\mathbf{F}}_A \\ \partial_t \hat{\mathbf{k}} &= -\frac{i}{\hbar} [\hat{\mathbf{k}}, \mathcal{H}_l + \mathcal{V}_{\text{ex}}] + D_B \nabla^2 \hat{\mathbf{k}} - \gamma_B \hat{\mathbf{k}} + \hat{\mathbf{F}}_B.\end{aligned}\quad (23)$$

Here we assume standard noble-gas pressures ( $10^{-1}$ – $10^4$  Torr), for which frequent collisions with the noble-gas atoms render the thermal motion diffusive, as described by the diffusion terms  $D_A \nabla^2 \hat{\mathbf{f}}$  and  $D_B \nabla^2 \hat{\mathbf{k}}$  [40]. For polarized alkali vapor, the interaction-free Hamiltonian from Eq. (10) has the simple form  $\mathcal{H}_0 = \hbar \int d^3 \mathbf{r} [\tilde{\omega}_A \hat{f}_z(\mathbf{r}, t) + \tilde{\omega}_B \hat{k}_z(\mathbf{r}, t)]$ , and  $\mathcal{V}_{\text{ex}}$  is given in Eq. (22). We emphasize that this model can describe the evolution of many-body quantum spin states.

The expressions in Eq. (23) encapsulate the various spin dissipation mechanisms into the relaxation rates  $\gamma_A$  and  $\gamma_B$ , given in Eqs. (2) and (3). Because of negligible noble-gas–cell-wall coupling, the diffusion-induced decay of the spatially uniform mode of the noble gas vanishes [40]. The incoherent spin-transfer terms [third term in the expressions in Eq. (21)], which have a negligible effect on the coherent dynamics, are omitted for brevity.

The Langevin noise operators  $\hat{\mathbf{F}}_A$  and  $\hat{\mathbf{F}}_B$  in Eq. (23) account for fluctuations and for preserving commutation relations under the relaxations  $\gamma_A$  and  $\gamma_B$  and diffusion [42].

As described in Sec. A, we consider highly polarized ensembles with most spins pointing downwards ( $-\hat{z}$ ) [1–3], and therefore approximate the local spin operators  $f_z = -p_A n_A q / 2$  and  $k_z = -p_B n_B / 2$ , and apply the Holstein-Primakoff transformation [2] to represent the collective states as excitations of a bosonic field with *local* annihilation operators

$$\begin{aligned}\hat{a}(\mathbf{r}, t) &= \hat{f}_-(\mathbf{r}, t) / \sqrt{2|f_z|}, \\ \hat{b}(\mathbf{r}, t) &= \hat{k}_-(\mathbf{r}, t) / \sqrt{2|k_z|}.\end{aligned}\quad (24)$$

The creation operators  $\hat{a}^\dagger(\mathbf{r}, t)$  and  $\hat{b}^\dagger(\mathbf{r}, t)$  flip upwards one alkali or noble-gas spin at position  $\mathbf{r}$ .

When the two gases are polarized, the energy cost of flipping a spin in one species is the sum of the Zeeman shift (due to the external magnetic field) and the so-called collisional shift (due to the effective magnetic field induced by the other species) [38]. The altered Larmor frequencies  $\omega_A = \tilde{\omega}_A - \zeta p_B n_B / 2$  and  $\omega_B = \tilde{\omega}_B - \zeta p_A n_A q / 2$  are obtained when the expressions in Eq. (23) are rewritten in



terms of  $\hat{a}(\mathbf{r}, t)$  and  $\hat{b}(\mathbf{r}, t)$ :

$$\begin{aligned}\partial_t \hat{a} &= -(i\omega_A + \gamma_A - D_A \nabla^2) \hat{a} - iJ \hat{b} + \hat{F}_A, \\ \partial_t \hat{b} &= -(i\omega_B + \gamma_B - D_B \nabla^2) \hat{b} - iJ \hat{a} + \hat{F}_B.\end{aligned}\quad (25)$$

Importantly, here we obtain the coherent spin-exchange rate

$$J = \zeta \sqrt{q p_A p_B n_A n_B} / 2, \quad (26)$$

which generalizes the coherent coupling rate in Eq. (8) for nonzero  $I$  and general spin polarizations  $p_A$  and  $p_B$ . This rate is responsible for the local exchange coupling of the two collective spins, as illustrated in Fig. 1(c). Notably,  $J$  is proportional to the square root of the atomic densities, which implies that the coupling is collective and benefits from collective enhancement.

The irreversibility of the evolution in Eq. (25) is dominated by alkali-spin relaxation and by spatial atomic diffusion. In principle, absence the diffusion, the dynamics of  $\hat{a}(\mathbf{r}, t)$  and  $\hat{b}(\mathbf{r}, t)$  at any location  $\mathbf{r}$  would be unitary and deterministic for short times  $t \ll (\gamma_A + \gamma_B)^{-1}$ . That could allow local (multimode) coupling of the two gases, owing to the locality of the collisional interaction. In practice, however, the diffusion term is dominant in the dynamics of the spin gases [43]. It is therefore fruitful to consider the spatial modes  $\hat{a}_m(t) \equiv \int A_m(\mathbf{r}) \hat{a}(\mathbf{r}, t) d^3\mathbf{r}$  and  $\hat{b}_n(t) \equiv \int B_n(\mathbf{r}) \hat{b}(\mathbf{r}, t) d^3\mathbf{r}$ , associated with orthonormal and complete sets of eigenmodes  $A_m(\mathbf{r})$  and  $B_n(\mathbf{r})$  of the respective diffusion-relaxation operators  $D_A \nabla^2 - \gamma_A$  and  $D_B \nabla^2 - \gamma_B$ . The modes  $A_m(\mathbf{r})$  and  $B_n(\mathbf{r})$  are determined by the cell's geometry and the wall boundary condition for the spins at the wall; see Refs. [40,44]. Typically one could assume partial or full relaxation of alkali spins by the cell walls (Robin boundary conditions) and no relaxation of noble-gas spins at the walls. The corresponding eigenvalues  $\gamma_{Am}$  and  $\gamma_{Bn}$  associate a decay rate with each mode.

The dynamics of the spatial modes  $\hat{a}_m$  and  $\hat{b}_n$ , illustrated in Fig. 1(d), is described by the coupled-mode equations

$$\begin{aligned}\partial_t \hat{a}_m &= -(i\omega_A + \gamma_{Am}) \hat{a}_m - iJ \sum_n c_{mn} \hat{b}_n + \hat{F}_{Am}, \\ \partial_t \hat{b}_n &= -(i\omega_B + \gamma_{Bn}) \hat{b}_n - iJ \sum_m c_{mn}^* \hat{a}_m + \hat{F}_{Bn}\end{aligned}\quad (27)$$

with an effective coupling  $Jc_{mn}$  that is determined by their integrated spatial overlap coefficients  $c_{mn} = \int A_m(\mathbf{r}) B_n^*(\mathbf{r}) d^3\mathbf{r}$ , being elements of a unitary matrix. The noise terms  $\hat{F}_{Am}$  and  $\hat{F}_{Bn}$  and our protocol for numerical solutions of these equations are given in Appendix E.

## V. COUPLING REGIMES

To illustrate and consider the dynamics of the coupled quantum spin gases, we find it fruitful to consider a simple

and analytical two-mode approximation of Eq. (27). This solution describes the dynamics of the collective symmetric mode  $\hat{b}$  of the noble-gas spins and the symmetric mode of the alkali spins  $\hat{a}$  defined in Sec. A. This approximation corresponds to choosing  $A_0 = 1/\sqrt{V}$ , where  $V$  is the volume of the cell, and therefore to setting  $c_{ij} = \delta_{i0}\delta_{j0}$  in Eq. (27). The resulting simplified two-mode model is

$$\partial_t \hat{a} = -iJ \hat{b} + (i\Delta - \gamma) \hat{a} + \hat{F}_A, \quad (28a)$$

$$\partial_t \hat{b} = -iJ \hat{a}, \quad (28b)$$

where the alkali decay rate  $\gamma = \gamma_A + D_A \pi^2 / R^2$  incorporates the (approximate) effect of diffusion in a cell with radius  $R$ . These equations are written in a rotating frame of the noble-gas spins, where  $\Delta = (g_A - g_B)B + \Delta_c$  denotes the mismatch of precession frequencies of the two polarized gases, with  $g_A$  and  $g_B$  being the gyromagnetic ratios of the alkali and noble-gas spins. At zero magnetic field, the detuning is biased by the mean collisional shift  $\Delta_c = \zeta(p_A n_A q - p_B n_B) / 2$  due to the difference in the effective magnetic fields induced by one species on the other [38].  $\hat{F}_A$  is the quantum noise operator (given in Appendix C). The decay of the noble-gas spins is omitted here as we are interested in timescales much shorter than their (hours-long) decoherence time.

With the coupling rate  $J$ , detuning  $\Delta$ , and relaxation  $\gamma$ , Eq. (28) has the canonical form of a coupled two-mode system [2]. While  $J$  cannot be varied rapidly,  $\Delta(B)$  can be controlled efficiently by variation of the external magnetic field  $B$  along the polarization axis.  $B$  alters  $\Delta$  by predominantly altering the precession frequency of the alkali spins, owing to the 100-fold to 1000-fold difference in the gyromagnetic ratios  $g_A$  and  $g_B$ . When the interaction is set off resonance  $|\Delta(B)| \gg J, \gamma$ , the two collective spins effectively decouple. This decoupling is often used in sensing applications to diminish the effect of the alkali on the noble-gas dynamics [30,45–47]. In this regime, the alkali and noble-gas spins precess independently; the alkali spin experiences fast relaxation at rate  $\gamma$ , while the noble-gas spin maintains its long coherence time. We simulate these dynamics first for coherent spin states, as shown in Fig. 3(a).

Conversely, when the magnetic field is tuned to the so-called compensation point  $\Delta(B) = 0$  [48], the interaction becomes resonant, and the two spin ensembles hybridize. The magnetic field thus acts as a controllable switch, rapidly coupling or decoupling the two spin ensembles. Romalis and coworkers demonstrated the alkali–noble-gas hybridization in the critically damped regime  $\gamma \gtrsim J, |\Delta|$  [48]. In this regime, the noble-gas spins inherit a large fraction of the alkali spins' decoherence rate and thus thermalize before the transfer of excitations is complete, as shown in Fig. 3(b). The overdamped regime features

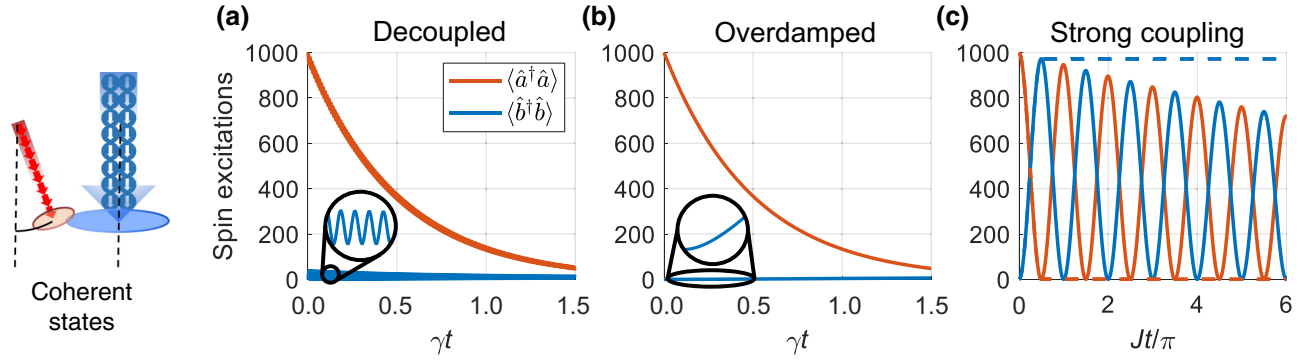


FIG. 3. Evolution of spin excitations of interacting alkali and noble-gas ensembles in different coupling regimes. Both ensembles are initialized in coherent spin states, with the alkali spins initially having  $\langle \hat{a}^\dagger \hat{a} \rangle = 1000$  excitations and the noble-gas spins in the vacuum state  $\langle \hat{b}^\dagger \hat{b} \rangle = 0$ . (a) Decoupled modes. At large detunings  $\Delta = 10J = 600\gamma$ , the spin ensembles are decoupled, and the alkali excitations decay at rate  $\gamma$ . The noble-gas spins exhibit negligible exchange with the alkali spins (inset). (b) Overdamped coupling. At  $\Delta = 0$ , the alkali and noble-gas spins hybridize and decay, here at rate  $\gamma = 10J$ , exhibiting partial transfer of the excitations (inset). (c) Strong coupling. The periodic exchange for  $J = 57\gamma$  at  $\Delta = 0$  allows coherent transfer of spin excitations. Application of a large magnetic field at  $t = \pi/2J$  decouples the spin ensembles and “stores” the excitations in the noble-gas spin state (dashed line).

a large enhancement in the sensitivity to various external fields and enables the operation as a comagnetometer sensor [48,49].

Here we focus on the recently demonstrated regime  $J \gg \gamma$ , which we identify as *strong coupling* [29]. In this regime, the evolution is governed by the beam-splitter Hamiltonian  $\hbar J(\hat{a}^\dagger \hat{b} + \hat{b}^\dagger \hat{a})$ , which leads to the exchange of quantum states between the spin ensembles. This is illustrated in Fig. 3(c) for coherent states, demonstrating a coherent transfer of spin excitations, as recently observed [29]. One can dynamically tune the exchange rate by varying the magnetic field strength. In particular, maintaining the resonance condition  $\Delta(B) = 0$  for duration  $t = \pi/2J$  and subsequently ramping  $B$  up to  $\Delta \gg J$  yields a deterministic state transfer between the two ensembles akin to a  $\pi$  pulse.

The accumulated effect of the spin-exchange collisions is coherent only as long as their *incoherent* contribution is negligible. As described by the incoherent-transfer term in Eq. (1), spin-exchange collisions introduce an additional relaxation rate  $k_{SE}n_B/q$  into the alkali spin rotation  $\gamma$ . Consequently, since  $n_B \gg n_A$ , the strong-coupling condition  $J \gg \gamma$  requires that the precession angle  $\langle \phi \rangle$  remains very small,  $\langle \phi \rangle \ll \sqrt{q p_A p_B} \sqrt{n_A/n_B} < 1$ . Thus, strong coupling of the spin ensembles relies on the weakness of the individual spin-exchange collisions.

## VI. EXAMPLES AND APPLICATIONS

In this section, we analyze the exchange process between the alkali and noble-gas spins in the strong-coupling regime ( $J \gg \gamma$ ). We consider the case in which the alkali spin is initialized in a nonclassical state and characterize the state of the noble-gas spin by the end of the exchange. We first demonstrate the exchange for the

quintessential case of a Fock state in Sec. VI A using the two-mode approximation. We analyze the exchange of a spin-squeezed state in Sec. VI B, and in Sec. VI C we discuss its potential use for quantum meteorology applications.

### A. Exchange of Fock states

We consider a system initialized in the state

$$|\psi(0)\rangle = |m\rangle_A |0\rangle_B = \frac{1}{\sqrt{m!}} (\hat{a}^\dagger)^m |0\rangle_A |0\rangle_B, \quad (29)$$

where the collective spin of the noble gas is in its vacuum spin state  $|0\rangle_B$ , and the collective spin of the alkali is initialized in the  $m$ th Fock state, a symmetric superposition with exactly  $m \ll N_A$  alkali spins pointing upwards. The simple exchange we consider corresponds to a resonant transfer, in which for a short duration  $T_\pi = \pi/2J$  the magnetic field is set to satisfy  $\Delta(B) = 0$ . Once the exchange is complete, setting  $\Delta(B) \gg J$ ,  $\gamma$  decouples the two spin gases and renders the noble-gas spin rotation induced by the alkali spin  $\gamma J^2/\Delta^2$  negligible (i.e., much smaller than the induced relaxation rate  $\gamma/2$  under the strong-coupling conditions).

Using the two-mode solution [see Eq. (F3), which is the integral version of Eq. (28) in the strong-coupling limit], we substitute the time-dependent operator  $\hat{a}(t)$  and find that the state of the system at any time  $0 \leq t \leq T_\pi$  is given by

$$|\psi(t)\rangle = \alpha(t)|\bar{\psi}(t)\rangle + \beta(t)|\delta\psi(t)\rangle, \quad (30)$$

where  $|\bar{\psi}\rangle$  is a symmetric quantum state, composed of multiples of the symmetric operators  $\hat{a}$  and  $\hat{b}$ , and  $|\delta\psi\rangle$  is an undesired state, composed of nonsymmetric superpositions into which the system might evolve due to relaxation and

quantum noise. For the exchange of the Fock state, we find

$$\alpha(t)|\bar{\psi}(t)\rangle = [\hat{U}(t)]^m |0\rangle_A |0\rangle_B, \quad (31)$$

with

$$\hat{U}(t) \equiv e^{-\gamma t/2} [\cos(Jt)\hat{a}^\dagger + i \sin(Jt)\hat{b}^\dagger], \quad (32)$$

whereas the stochastic term is given by

$$\beta(t)|\delta\psi\rangle = \prod_{k=0}^{m-1} (\hat{w}_B^\dagger)^{k+1} [\hat{U}(t)]^{m-k} |0\rangle_A |0\rangle_B. \quad (33)$$

The properties of the quantum noise operator  $\hat{w}_B^\dagger$ , which describes excitations of nonsymmetric spin modes, are derived in Appendix F.

At  $t = T_\pi$ , the collective Fock state is transferred to the noble-gas spins, and the symmetric part of the wave function becomes

$$|\bar{\psi}(T_\pi)\rangle = |0\rangle_A |m\rangle_B \quad (34)$$

with a high transfer fidelity of  $|\alpha(T_\pi)|^2 = 1 - m\pi\gamma/2J$  to first order in  $\gamma/J$ . Despite the stochastic nature of the collisional coupling, the state transfer leaves the alkali in the vacuum spin state except for the small contribution due to noise processes  $|\beta|^2 = 1 - |\alpha|^2$ . Moreover, at intermediate times, the two spin gases become entangled, with maximal entanglement obtained at  $t = T_\pi/2$ . For example, if the alkali is initialized with a single spin excitation ( $m = 1$ ), the symmetric wave function becomes

$$|\bar{\psi}(T_\pi/2)\rangle = (|1\rangle_A |0\rangle_B + i |0\rangle_A |1\rangle_B) / \sqrt{2}, \quad (35)$$

which manifests entanglement between the two spin ensembles with fidelity  $|\alpha(T_\pi/2)|^2 = 1 - \pi\gamma/4J$ .

We illustrate the exchange dynamics in Fig. 4(a) using the two-mode approximation with  $J = 55\gamma$ . The alkali spin ensemble is initialized in a Fock state with two spin excitations, and the noble-gas spin is initialized in a vacuum. We present  $|\alpha(t)|^2$ , which describes the probability of transferring the two excitations to the uniform mode of the noble-gas spin and leaving the alkali spin in the vacuum state, i.e.,  $|\langle\psi(t)|(|0\rangle_A |2\rangle_B)\rangle|^2$ . Here, by changing  $\Delta$  at  $t = \pi/2J$ , the excitation transfer is complete, and the noble-gas spin becomes decoupled from the alkali spin and free from its induced relaxation (dotted black line).

### B. Exchange of a spin-squeezed state

We now consider the exchange of spin squeezing from the alkali to the noble gas. The initial state of the system is

$$|\psi(0)\rangle = |\xi\rangle_A |0\rangle_B = e^{(\xi^* \hat{a}^2 - \xi \hat{a}^{\dagger 2})/2} |0\rangle_A |0\rangle_B, \quad (36)$$

where the alkali is in a vacuum squeezed state  $|\xi\rangle_A$ . We use  $\xi = |\xi|e^{i\theta}$  to denote the squeezing parameter, where

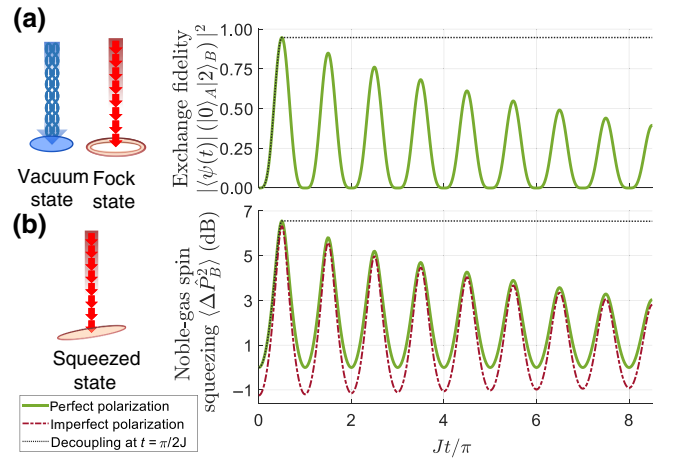


FIG. 4. Exchange of nonclassical states in the two-mode approximation. (a) Probability of finding the collective noble-gas spin with exactly two excitations (Fock state) and the alkali spin in a vacuum. The two ensembles are perfectly polarized ( $p_A = p_B = 1$ ), and the system is initiated with two excitations in the collective alkali spin. (b) Exchange of spin variance between the collective alkali spin quadrature  $\hat{X}_A$  and the collective noble-gas spin quadrature  $\hat{P}_B$ . The alkali spin variance  $\langle\Delta\hat{X}_A^2\rangle$  is initially squeezed by 7 dB. We present two cases: perfectly polarized spins ( $p_B = p_A = 1$ , green line), which correspond to an initial noble-gas spin variance  $\langle\Delta\hat{P}_B^2\rangle$  of 0 dB, and partially polarized spins ( $p_A = 0.95$  and  $p_B = 0.75$ , red line), which correspond to an initial noble-gas spin variance of  $-1.25$  dB. In both cases, the noble-gas spin is efficiently squeezed by the end of the exchange, interchanging its variance with the alkali spin. In both calculations, the magnetic field is tuned to resonance  $\Delta(B) = 0$  at  $t = 0$  to enable exchange, and we use  $J = 55\gamma$  for the perfectly polarized case. If the magnetic field is detuned at  $t = \pi/2J$ , the two ensembles are decoupled and the exchange is complete (dashed black line).

the magnitude  $|\xi|$  determines the degree of squeezing and the angle  $\theta/2$  determines its orientation in phase space [50]. For example, if  $\xi$  is real and  $\xi > 0$ , then the  $\hat{X}_A = (\hat{a} + \hat{a}^\dagger)/2$  quadrature is squeezed and its variance is given by  $\langle\Delta\hat{X}_A^2\rangle = \exp(-2\xi)/4$ , whereas the other quadrature  $\hat{P}_A = i(\hat{a}^\dagger - \hat{a})/2$  is antisqueezed, and its variance is given by  $\langle\Delta\hat{P}_A^2\rangle = \exp(2\xi)/4$ . For  $\xi = 0$ , this state becomes the vacuum state with variance  $1/4$  corresponding to the standard quantum limit. Note that we adopt the conventions for  $\hat{X}$  and  $\hat{P}$  from Ref. [50], whose variance is different by a factor of 2 with respect to the definitions in Ref. [2].

To describe the exchange, we first consider the evolution of the two ensembles for  $\gamma = 0$ , and then characterize the effect of relaxation and noise. In Appendix F [see Eq. (F7)], we derive the evolution of the system as a function of time and find that, by the end of the exchange, the spin squeezing is transferred to the collective spin of the noble gas:

$$|\psi(T_\pi)\rangle = e^{(-\xi^* \hat{b}^2 + \xi \hat{b}^{\dagger 2})/2} |0\rangle_A |0\rangle_B = |0\rangle_A |-\xi\rangle_B. \quad (37)$$

Therefore, the collective states of the noble-gas and alkali spins are exchanged but the spin-squeezed state of the noble gas is rotated in phase space by  $\pi/2$ . For an alkali spin initially squeezed along the  $\hat{X}_A$  quadrature with  $\xi > 0$ , it is the conjugate quadrature  $\hat{P}_B$  of the noble-gas spin that becomes squeezed with the same degree of squeezing [i.e.,  $\langle \Delta \hat{P}_B^2 \rangle = \exp(-2|\xi|)/4$ ], while  $\hat{X}_B$  becomes antisqueezed [i.e.,  $\langle \Delta \hat{X}_B^2 \rangle = \exp(2|\xi|)/4$ ]. The alkali ends up in the vacuum state, with the variances  $\langle \Delta \hat{X}_A^2 \rangle = \langle \Delta \hat{P}_A^2 \rangle = 1/4$ .

For finite  $\gamma$ , the transfer process is imperfect due to relaxation and coupling to nonsymmetric spin modes. For this case, we derive the evolution of the spin variances in Eq. (F12) and find that the noble-gas quadrature  $\hat{P}_B$  is partially squeezed at the end of the exchange, and that its variance to first order in  $\gamma/J$  is given by

$$\langle \Delta \hat{P}_B^2(T_\pi) \rangle = \frac{e^{-2\xi}}{4} + \frac{\pi\gamma}{8J} (1 - e^{-2\xi}). \quad (38)$$

Importantly, as shown in Fig. 5, for any initial alkali squeezing with  $\langle \Delta \hat{X}_A^2 \rangle < 1/4$ , the noble-gas variance  $\langle \Delta \hat{P}_B^2(T_\pi) \rangle$  is squeezed below the standard quantum limit. For weak-moderate squeezing with  $|\xi| \ll \log(\pi\gamma/2J)$ , the exchange is almost complete, and the effect of relaxation is negligible. For initially large squeezing, however, the noise originating from the alkali relaxation degrades the squeezing degree and limits the spin variance from any value below vacuum noise to a fraction  $(\pi\gamma/2J)$  of the vacuum noise. Notably, in the strong-coupling regime, this limit may be small, therefore still allowing the exchange of a high degree of spin squeezing.

It is also insightful to discuss the consequences of having nonperfect polarizations of the two spin gases. The trivial direct consequence of  $p_A, p_B < 1$  is the decrease of  $J$ , which scales down with  $\sqrt{p_A p_B}$ . In addition, the quantum noise processes for partially polarized ensembles deviate from vacuum statistics and correspond to thermal processes with about  $\bar{n}_I = (1-p)/2p$  incoherent excitations ( $p = p_{q|b}$ ) [see Eqs. (C8) and (C9)]. For moderate-high spin polarizations,  $\bar{n}_I \ll 1$ , and its effect on the exchange at short times is small.

Generally, partially polarized and even completely unpolarized spin ensembles can host nonclassical states whose spin variance is squeezed [2,18,51,52]. However, for nonunity spin polarization, there are several different metrics for spin squeezing of spin ensembles. Here we consider the metric proposed and analyzed in Ref. [2], which quantifies the variance of  $\langle \Delta \hat{P}_B^2 \rangle$  compared with  $1/4$ . For spin-1/2 noble gases, the collective spin variance  $\langle \Delta \hat{K}_y^2 \rangle$  is typically independent of the spin polarization. For example, noble-gas spins in the fully mixed state

$$\rho_b = \prod_{b=0}^{N_B} (p_B |\downarrow\rangle_b \langle \downarrow|_b + (1-p_B) |\uparrow\rangle_b \langle \uparrow|_b) \quad (39)$$

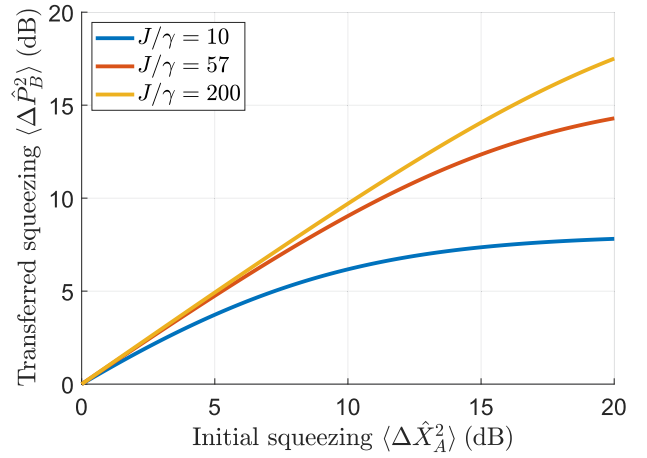


FIG. 5. Efficiency of spin-squeezing transfer. The collective alkali spin is initially squeezed along the  $\hat{X}_A$  quadrature, and the squeezing property is transferred to the  $\hat{P}_B$  quadrature of the collective noble-gas spin. After the transfer time  $T_\pi$ , the spins can be decoupled by application of a large magnetic field. The transfer of squeezing in decibels is almost ideal (linear dependence) for a low degree of squeezing, and its range is extended as the coupling between the gases becomes stronger (higher  $J/\gamma$ ). The graph is generated with Eq. (38) derived for the two-mode approximation.

have a collective spin variance  $\langle \Delta \hat{K}_y^2 \rangle = \text{Tr}(\rho_B \hat{K}_y^2) = N_B/4$ , which is independent of the degree of spin polarization. As  $\langle \Delta \hat{P}_B^2 \rangle = \langle \Delta \hat{K}_y^2 \rangle / N_B p_B$ , the initial noble-gas spin variance is inversely proportional to the spin polarization,  $\langle \Delta \hat{P}_B^2 \rangle = 1/4p_B$ , and for  $p_B < 1$  is increased with respect to the vacuum state. For alkali ensembles, the nonzero nuclear spin in each atom follows an internal spin-temperature distribution, which leads to a polarization-dependent variance of the collective spin,  $\langle \Delta \hat{F}_x^2 \rangle = N_A q/4$ , where the slowing-down factor  $q$  is given in Eq. (18) [41]. For unpolarized alkali spins, this variance is associated with the thermal spin-state variance [18]. Using  $\langle \Delta \hat{X}_A^2 \rangle = \langle \Delta \hat{K}_x^2 \rangle / q N_A p_A$ , we find that  $\langle \Delta \hat{X}_A^2 \rangle = 1/4p_A$  in partially polarized alkali ensembles.

In the strong-coupling regime, the collective exchange process conserves the total number of spin excitations  $\langle \hat{a}^\dagger \hat{a} + \hat{b}^\dagger \hat{b} \rangle$  and leads to exchange between the variances  $\langle \Delta \hat{P}_B^2 \rangle$  and  $\langle \Delta \hat{X}_A^2 \rangle$ . In Fig. 4(b), we present the transferred squeezed variance obtained by the noble-gas spin from an initially squeezed alkali spin, whose  $X_A$  quadrature is squeezed by 7 dB. We consider two cases: perfectly polarized ensembles ( $p_A = p_B = 1$ , green line) and imperfect polarization of the ensembles with  $p_A = 0.95$  and  $p_B = 0.75$  (red line). For the former case, the initial variance of the alkali is  $\langle \Delta \hat{X}_A^2 \rangle = 0.05$ , and the noble gas is in a vacuum state with initial variance  $\langle \Delta \hat{P}_B^2 \rangle = 0.25$ . For the latter case, initially  $\langle \Delta \hat{X}_A^2 \rangle = 0.053$  (squeezed by 7 dB with respect to its initial polarization  $1/4p_A$ ) and

$\langle \Delta \hat{P}_B^2 \rangle = 1/3$ . In both cases, the alkali's squeezed quadrature is transferred efficiently to the noble gas, enabling the exchange even for moderate spin polarizations. Changing  $\Delta$  at  $t = \pi/2J$  enables us to decouple the spin gases and maintain the squeezed quadrature at the noble-gas spin.

### C. Noble-gas magnetometry

The hybrid system of alkali and noble-gas spins can be used for various quantum sensing applications. In this subsection, we demonstrate potential increase of the fundamental projection noise sensitivity, attained by initial transfer of spin squeezing from the alkali to the noble-gas spins for a simplified magnetometer configuration using the two-mode approximation. Here we consider a sensor that is sensitive to low-frequency oscillating magnetic fields transverse to the polarization axis, in the form of  $B_\perp \cos \omega t$ , whose angular frequency  $\omega$  is resonant with the precession frequency of the noble gas  $\omega_B$ . This regime is relevant, for example, in new-physics searches for anomalous magnetic fields [53,54]. For simplicity of the analysis, we assume that both gases are spin polarized along  $\hat{z}$  (the alkali spins can be optically pumped continuously) and that the sensor operates in the detuned regime  $\Delta \gg J \gtrsim \gamma_A \gg \gamma_B$ .

We characterize the effect of transverse magnetic fields on the spin dynamics by adding the source terms  $iqg_{AP_A}N_A B_\perp/2$  and  $ig_{BP_B}N_B B_\perp/2$  to Eqs. (28a) and (28b), respectively. The numerical factors in these terms and the dependence on density and polarization (with respect to the mean-field Bloch equations) result directly from the definition of the operators  $\hat{a}$  and  $\hat{b}$ . In this analysis, we do not ignore the noble-gas relaxation rate  $\gamma_B$  and the associated quantum noise operator  $\hat{F}_B$ . For simplicity, we consider the limit in which the transverse magnetic field  $B_\perp$  tilts predominantly the noble-gas spins off axis and induces their precession, i.e., formally requiring a sufficiently large noble-gas magnetization  $g_B \sqrt{N_B p_B} \gg J g_A \sqrt{q N_A p_A} / |\Delta|$ . The alkali spin then responds predominantly to the noble-gas spin precession, which can be detected by optical means.

In operating the sensor, one estimates the magnitude of the magnetic field  $B_\perp$  using the integrated operator

$$\hat{M}(T) = \frac{1}{T} \int_0^T \sin(\omega t) \text{Re}(\hat{a}(t)) dt, \quad (40)$$

which captures the response of the alkali spins along  $x$  to the time-varying field in its rotating frame. This response is measured with a lock-in amplifier. Its mean value  $\langle \hat{M} \rangle$  is associated with the signal that is proportional to the magnetic field amplitude, and its variance  $\langle \Delta \hat{M}^2 \rangle$  is associated with noise. We solve the two-mode equations of motion in the time domain in Appendix G and find the temporal solution for  $\hat{a}(t)$  in Eq. (G3) as well as that for  $\hat{M}(T)$

in Eq. (G13). The solution for  $\hat{M}$  is composed of a deterministic term, which is governed by the response to the magnetic field signal, and two noise terms, which limit the magnetic sensitivity. Both noise terms are associated with the projection noise of the spin ensembles and, in turn, limit the fundamental sensitivity of the magnetometer. One noise term  $\delta B_{\text{init}}$  depends on the initial variance of the spin ensembles, and the other noise term  $\delta B_F$  is governed by the effective thermalization rate of the long-lived spin mode of the noble gas:  $\tilde{\gamma}_B = \gamma_B + J^2 \gamma_A / \Delta^2$ .

In Fig. 6, we plot (in normalized units) the contribution of the two noise terms to the total sensitivity

$$\delta B_{\text{tot}} = \sqrt{\delta B_{\text{init}}^2 + \delta B_F^2} \quad (41)$$

as derived in Appendix G. At short times  $T \ll \tilde{\gamma}_B^{-1}$ , the term  $\delta B_{\text{init}}$  is dominant, resulting in a magnetic sensitivity given by

$$\delta B_{\text{init}} = \frac{8}{g_B T} \sqrt{\frac{\langle \Delta \hat{P}_B^2 \rangle + \frac{J^2}{\Delta^2} \langle \Delta \hat{P}_A^2 \rangle}{N_B p_B}}. \quad (42)$$

In the detuned limit we consider  $J \ll |\Delta|$ ; this noise is predominantly governed by the initial spin variance of the noble gas. Initializing the noble gas with a spin-squeezed quadrature  $\hat{P}_B$  therefore decreases its variance  $\langle \Delta \hat{P}_B^2 \rangle$  and results in greater sensitivity than with nonsqueezed noble-gas spins. The contribution of  $\delta B_F$ , which arises due to infiltration of noise, cannot be further reduced by spin squeezing (as the noise causes decoherence of this state), and the net accuracy increase is presented as the shaded light-blue area in Fig. 6. At longer times  $T \gg \tilde{\gamma}_B^{-1}$ , the uniform mode of the noble-gas spin decoheres, rendering its initial state unimportant with respect to the coupled noise, which sets the sensitivity to be

$$\delta B_F = \frac{1}{8g_B} \sqrt{\frac{\tilde{\gamma}_B}{T N_B p_B}}. \quad (43)$$

Notably, on short time scales, readout noise averages out with  $1/T$  scaling, whereas, on longer time scales, averaging is slower and scales as  $1/\sqrt{T}$ . The threshold between the two regimes is set by the timescale  $\tilde{\gamma}_B^{-1}$ , which can be prolonged up to the very long  $\gamma_B^{-1}$  by increasing the relative detuning  $\Delta$  and decreasing the contribution of the alkali spins to the noble-gas relaxation (being the motivation for detuned operation). The above analysis might be generalized for other noble-gas sensors such as comagnetometers and rotation sensors [45,47,49].

## VII. NUMERICAL SOLUTION

In this section, we present the numerical solution for the exchange of Fock and spin-squeezed states using the

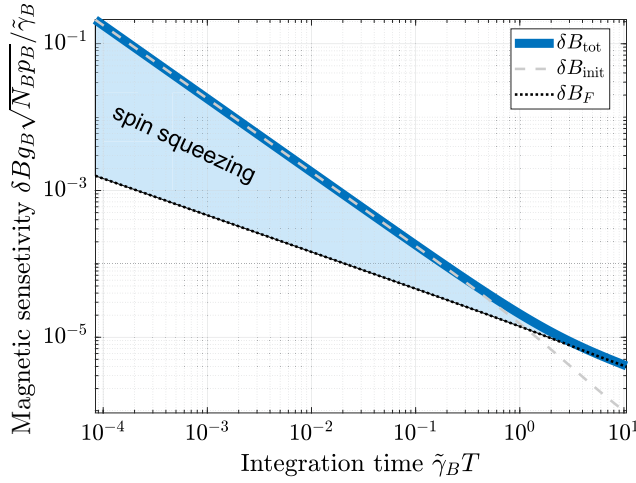


FIG. 6. Fundamental sensitivity of a hybrid alkali–noble-gas magnetometer. The magnetometer operates in the detuned limit  $\Delta \gg J$  and measures a low-frequency oscillating magnetic field  $B_{\perp} \cos \omega t$  near the resonance frequency of the noble gas. The magnetometer sensitivity is limited by atom projection noise of the two gases, which can be decomposed into two qualitatively different terms,  $\delta B_{\text{init}}$  and  $\delta B_F$ . At short times  $T \ll \tilde{\gamma}_B^{-1}$ , the limit is set by  $\delta B_{\text{init}}$  due to the variance of the initial state. This variance can be improved by initial squeezing of the noble-gas spins (shaded light-blue area). At longer times  $T \gg \tilde{\gamma}_B^{-1}$ , the sensitivity is limited by the decoherence of the noble-gas spins via the term  $\delta B_F$ . The decoherence rate  $\tilde{\gamma}_B = \gamma_B + J^2 \gamma_A / \Delta^2$  is the total decoherence rate of the noble-gas spins when they are coupled to the alkali spins in the detuned regime. The integration time and sensitivity are both presented in normalized units.

detailed model, demonstrating the multimode evolution of Eq. (27). We first present in detail the physical conditions we consider in the calculation and then analyze the evolution.

### A. Physical parameters

The parameters we use for the calculations are estimated for a mixture of  $^{39}\text{K}$  and  $^3\text{He}$  in a 2-in.-diameter spherical cell. To maximize the collective coupling rate  $J$ , we consider reasonably high densities of  $n_A = 3 \times 10^{14} \text{ cm}^{-3}$  (vapor pressure at 215 °C) and  $n_B = 2 \times 10^{20} \text{ cm}^{-3}$  (7.5 atm) and 30 Torr of  $\text{N}_2$  for quenching [48]. By standard optical pumping, the alkali spin polarization can be initialized in a spin-temperature distribution with  $p_A \geq 0.95$ , for which the slowing-down factor  $q$  is 4.1 [2,55]. The noble-gas spin can be initialized via SEOP to a moderate yet sufficient polarization of  $p_B \gtrsim 0.75$  [56].

A coupling rate of  $J = 1000 \text{ s}^{-1}$  is reached at this temperature, as  $v\sigma\langle\phi\rangle = 2 \times 10^{-14} \text{ cm}^3/\text{s}$  (corresponding to  $\langle\phi\rangle^2 \approx \langle\phi^2\rangle \approx 2 \times 10^{-10} \text{ rad}^2$ ). The resonance condition  $\Delta = (g_a - g_B)B + \Delta_c = 0$  is obtained for a magnetic field  $B = 94 \text{ mG}$ , predominantly compensating for the large collisional shift  $v\sigma\langle\phi\rangle p_B n_B / 2q$  experienced

by the potassium, and yielding the Larmor frequency  $g_B B = g_A B + \Delta_c = 300(2\pi) \text{ Hz}$ . The high alkali density and polarization and the relatively small Larmor frequency puts the potassium spins in the “spin-exchange relaxation-free” regime [57–59], rendering their relaxation via spin-exchange collisions negligible. The relaxation rate is governed by spin-rotation interaction with  $^3\text{He}$  and  $\text{N}_2$  and by spin-destruction collisions with other potassium atoms, giving  $\gamma = 17.5 \text{ s}^{-1}$  [11]. We thus reach the strong-coupling regime with potentially  $J > 55\gamma$ .

The spin state of  $^3\text{He}$  in this system can endure for 100 h, providing that magnetic field gradients, magnetic impurities in the cell, and alkali-induced dephasing are minimized [23,34,60]. The alkali spins can be initialized in a nonclassical state via entanglement-generation schemes [1,15] or by mapping nonclassical light onto the spin orientation moment [61].

### B. Multimode exchange

We numerically solve the multimode differential equation Eq. (27) to describe the exchange of two excitations (Fock state) and of a spin-squeezed state, with initial conditions similar to those for the two-mode approximation presented in Fig. 4. These calculations, however, account for the spatial dynamics with multiple diffusion modes [40]. The alkali spin is initialized with excitations of only its spatially symmetric (uniform) mode. As we assume completely depolarizing walls for the alkali, the uniform mode of the alkali is not an eigenmode of the diffusion operator. We use the first 200 spherically symmetric least-decaying modes of each spin ensemble to capture the coherent multimode dynamics of the spin gases. While the number of coupled diffusion modes is very large, we truncate high-order modes whose decoherence (including diffusion) is much larger than the coupling rate  $J$ . For the relatively large cell, high buffer gas pressure (corresponding to  $D_A = 0.054 \text{ cm}^2/\text{s}$  and  $D_B = 0.023 \text{ cm}^2/\text{s}$ ), and the strong coupled dynamic we consider here, there are tens of stable modes that coherently participate in the dynamics. To capture the effect of the truncated modes on the dynamics, we strictly approximate them as reservoir modes that do not contribute to the coherent process and only increase the relaxation and quantum noise [see Eq. (E2)]. We have verified the convergence for this choice of truncation.

We further include the effect of imperfect polarizations  $p_A = 0.95$  and  $p_B = 0.75$  by using a nonpure density matrix  $\rho$  for the multiple diffusion modes. This matrix is initialized with incoherent spin excitations of  $\langle \hat{a}_m^\dagger \hat{a}_m \rangle = 0.05$  and  $\langle \hat{b}_m^\dagger \hat{b}_m \rangle = 0.17$  at  $t = 0$  for each of the  $1 \leq m \leq 200$  modes we compute. We further include the increased quantum noise due to imperfect polarization as given in Eqs. (C8) and (C9) and calculate expectation values by tracing over the contribution of all diffusion modes. The results of the calculations are presented in Fig. 7. For

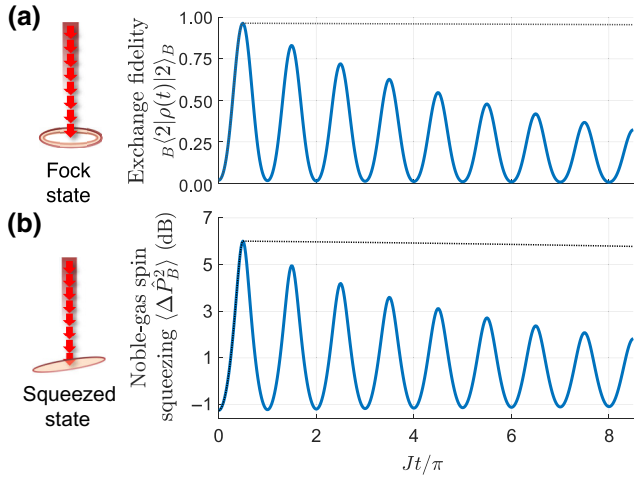


FIG. 7. Exchange of nonclassical states between partially polarized alkali and noble-gas spin ensembles using the multimode evolution. The exchange is calculated for the proposed experimental parameters and assuming the initial excitation is spatially uniform. This solution accounts for the effect of higher spatial modes and imperfect polarization with  $p_A = 0.95$  and  $p_B = 0.75$ . At  $t = 0$ , the magnetic field is tuned to resonance,  $\Delta(B) = 0$ . Detuning at  $t = \pi/2J$  decouples the two ensembles and completes the transfer (dotted black line, using  $B = 180$  mG). (a) Probability of populating the uniform (longest-lived) diffusion mode of the noble-gas spin with exactly two excitations (Fock state) when the system is initialized with two excitations in the alkali’s uniform mode. In contrast to Fig. 4, the fidelity presented here poses no conditions on the state of the alkali spin. (b) Exchange of squeezing with the alkali, which is initially spin squeezed by 7 dB. For both cases, the multimode evolution results in a faster decay rate over the two-mode approximation.

the exchange of the Fock state in Fig. 7(a), we present the fidelity of having exactly two excitations in the uniform mode of the noble-gas spin. This metric is different from that used in Fig. 4 by placing no requirement on the number of alkali-spin excitations during the exchange. For both the squeezing and the Fock state exchange, the multimode evolution results in only a finite increase of the relaxation rate and is qualitatively similar to the two-mode approximation.

## VIII. DISCUSSION

We present analytical and numerical quantum-mechanical models for the hybrid system of alkali-metal and noble-gas spins. The models reveal a collective mechanism that couples the macroscopic quantum states of the two spin ensembles. We highlight feasible experimental parameters for reaching the strong-coupling regime, which enables a faithful quantum-state transfer between the alkali and noble-gas ensembles.

It is intriguing that weak collisions, despite their random nature, allow an efficient, reversible, and controllable

exchange of excitations. It is particularly counterintuitive that this exchange preserves the unique quantum statistics of nonclassical states. Equations (28a) and (28b) manifest a genuine quantum interface, as they describe the exchange between the operators  $\hat{a}$  and  $\hat{b}$ , which in turn encapsulate the full quantum statistics of the collective spin states. The effect of the randomness of collisions on the quantum statistics is then incorporated in the noise operator  $\hat{F}_A$ .

In stochastic quantum systems, the variance of quantum noise satisfies  $\langle \hat{F}_A \hat{F}_A^\dagger \rangle \geq 2\gamma$  for any relaxation rate  $\gamma$ , where equality is obtained for the case of vacuum noise [42]. For perfect spin polarization, we find that the noise due to spin-exchange collisions is a vacuum noise, i.e., the minimal possible for an open quantum system (see Appendix C). This result is apparent, for example, in the exchange of a single spin excitation between perfectly polarized ensembles, where we obtain  $\langle \hat{F}_A \hat{F}_A^\dagger \rangle = \epsilon^2/t = 2\gamma$ .

While it is experimentally possible to approach unity polarization of the alkali atoms  $p_A \rightarrow 1$  [62,63], the highest  $^3\text{He}$  polarization demonstrated to date is  $p_B = 0.85$  [56]. It is therefore insightful to discuss the consequences of imperfect spin polarization  $p_A, p_B < 1$ . The first and more trivial consequence is a moderate reduction of  $J \propto \sqrt{p_A p_B}$ , since now only a fraction  $p_A p_B$  of the atomic collisions contribute to the collective exchange process. The second consequence is added noise due to the initial incoherent population of transverse spin excitations. These incoherent excitations are distributed over a macroscopic number of spatial modes. Therefore, despite having a macroscopic number of depolarized atoms, the number of excitations per mode can be small. Notably, for a finite polarization degree  $0 < p \leq 1$ , the mean number of incoherent excitations in the uniform spatial mode is given by  $\bar{n}_I = (1-p)/2p$ . For  $p$  close to unity,  $\bar{n}_I \ll 1$  is small. Finally, the incoherent excitations residing in all other modes form a “thermal reservoir” of spins that is manifested as excess quantum noise. In particular, the collisional coupling of the collective spin to this reservoir increases the variance of the quantum noise operators acting on the spin. This noise is accumulated during the dynamics and is thus small at short timescales. Importantly, the overall effects of excess noise for spin ensembles with polarization of tens-of-percent is relatively small.

The quantum interface we study allows a controllable state exchange between two spin-gas species, and it is of particular importance when it comes to noble-gas spins, which are extremely long-lived but optically inaccessible. The interface can reach the strong-coupling regime and allows nonadiabatic exchange, thus significantly increasing operation bandwidth. In conjunction with recent experiments demonstrating the coherent, efficient, and bidirectional properties of the collective coupling in the classical regime [29,30], our study thus opens a path to couple light to the transparent spins in the quantum regime. The

scenario resembles quantum-logic operations with nuclear ensembles in solids, where a long-lived nuclear spin is accessible via the hyperfine interaction with an electron spin, which is optically manipulated and interrogated [64]. Here, however, the collective spins of the two gases form two coupled quantum oscillators—one that is optically accessible and another that is long-lived—which can be used for various quantum information applications with continuous variables [65,66]. The spin-exchange interface therefore paves the way toward wider applications of noble-gas spins in quantum optics, including long-lived quantum memories and long-distance entanglement under ambient conditions [31–33], as well as to fundamental research on the limits of quantum theory for entangled macroscopic objects.

### ACKNOWLEDGMENTS

We thank C. Avinadav for helpful discussions. We acknowledge financial support by the Israel Science Foundation and ICORE, the European Research Council starting investigator grant Q-PHOTONICS 678674, the Pazy Foundation, the Minerva Foundation with funding from the German Ministry for Education and Research, and the Laboratory in Memory of Leon and Blacky Broder. O.K. and R.S. contributed equally to this work.

### APPENDIX A: STOCHASTIC EVOLUTION OF A SINGLE EXCITATION

For a system initialized with a symmetric excitation  $|\psi_0\rangle = |1\rangle_A|0\rangle_B$ , for short timescales and to first order in  $\phi$ , the evolution by Eq. (6) is given by

$$|\psi(t/\tau)\rangle = \left[ \mathbb{1} - i \sum_n \sum_{ab} \varkappa_{ab}^{(n)} \phi_a^{(n)} \left( \frac{1}{2} \hat{s}_a^- \hat{k}_b^+ + \hat{s}_{az} \hat{k}_{bz} \right) \right] |\psi_0\rangle,$$

using  $\hat{s}_a^+ \hat{k}_b^- |\psi_0\rangle = 0$  (since no excitations populate the initial state of the noble gas). The second term is then decomposed into the deterministic and stochastic terms,  $-iJt|1\rangle_A|0\rangle_B$  and  $-i\epsilon|\delta\psi\rangle$ , as outlined in the main text. Here we identify the stochastic transition amplitude

$$\epsilon = \left[ \sum_b \left( \sum_a \sum_{n=0}^{t/\tau} \delta\phi_{ab}^{(n)} \right)^2 / 2N_A \right]^{1/2} \quad (\text{A1})$$

and the stochastic wave function

$$|\delta\psi\rangle \equiv |0\rangle_A|\delta\psi\rangle_B + |\delta\psi\rangle_A|0\rangle_B, \quad (\text{A2})$$

where

$$\epsilon|\delta\psi\rangle_B = \frac{1}{2\sqrt{N_A}} \sum_b \left[ \sum_{an} \delta\phi_{ab}^{(n)} \right] \hat{k}_b^+ |0\rangle_B \quad (\text{A3})$$

describes stochastic nonsymmetric noble-gas spin excitations, while

$$\epsilon|\delta\psi\rangle_A = \frac{1}{2\sqrt{N_A}} \sum_a \left[ \sum_{bn} \delta\phi_{ab}^{(n)} \right] \hat{s}_a^+ |0\rangle_A \quad (\text{A4})$$

describes nonsymmetric excitations of alkali spins. These wave functions depend on the fluctuation of the spin precession  $\delta\phi_{ab}^{(n)} = \varkappa_{ab}^{(n)} \phi_a^{(n)} - \langle\phi\rangle/N_B$ , where  $\langle\phi\rangle \equiv \langle\phi_a^{(n)}\rangle$ . Following the central-limit theorem and assuming the stringent condition that any two collisions are uncorrelated  $\langle\delta\phi_{a'b}^{(n')}\delta\phi_{ab}^{(n)}\rangle = \delta_{aa'}\delta_{bb'}\delta_{nn'}\langle(\delta\phi_{ab}^{(n)})^2\rangle$ , we find the result in the main text  $\epsilon \rightarrow \sqrt{\langle\phi^2\rangle t/2\tau}$ , where  $\langle\phi^2\rangle \equiv \langle[\phi_a^{(n)}]^2\rangle$ .

### APPENDIX B: COLLISION STATISTICS

Here we present details of the collision statistics of alkali and noble-gas atoms used in the derivation of the expressions in Eq. (21) from expressions in Eq. (17), as well as for characterization of the spin-exchange noise in Eq. (C1).

The microscopic parameter  $\varkappa_{ab}(t, \tau)$  indicates if the pair  $a$ - $b$  has collided during the time interval  $[t, t + \tau]$  by

$$\varkappa_{ab}(t, \tau) = \int_t^{t+\tau} \delta(s - t_{ab}^{(i)}) ds. \quad (\text{B1})$$

For short  $\tau$ , we can assume a ballistic motion of the particles, such that the two-body displacement satisfies

$$\mathbf{r}_{ab}(t+s) = \mathbf{r}_{ab}(t) - \mathbf{v}_{ab}(t)s \quad (\text{B2})$$

for any  $s \in [t, t + \tau]$ . A collision of the pair occurs at  $t_{ab}^{(i)}$  if  $r_{ab}(t_{ab}^{(i)}) \leq \epsilon$ , where  $\epsilon$  characterizes the hard-sphere radius of the pair, satisfying  $\sigma = \pi\epsilon^2$  and  $r_{ab} = |\mathbf{r}_{ab}|$ . The time of a collision is then determined by

$$|\mathbf{r}_{ab}(t) - \mathbf{v}_{ab}(t_{ab}^{(i)} - t)| \leq \epsilon.$$

Solving for  $t_{ab}^{(i)}$ , we obtain the expression

$$t_{ab}^{(i)} = t + \frac{r_{ab}(t)}{v_{ab}} \left( \cos\theta_{ab}^v \pm \sqrt{\epsilon^2/r_{ab}^2(t) - \sin^2\theta_{ab}^v} \right), \quad (\text{B3})$$

where  $\theta_{ab}^v \in [0, \pi]$  is the relative angle between  $\mathbf{r}_{ab}$  and  $\mathbf{v}_{ab}$ . Therefore,  $t_{ab}$  exists only if  $\sin^2\theta_{ab}^v \leq \epsilon^2/r_{ab}^2(t)$ . Since  $\epsilon$  is about a few angstroms, collisions occur only at small angles  $\theta_{ab}^v \ll 1$ . Ignoring the collision duration  $\tau_c \lesssim 2\epsilon/v_{ab} \ll \tau$ , we can approximate the collision time as the average of the two solutions, yielding  $t_{ab}^{(i)} = t + r_{ab}(t)/v_{ab}$ , if  $\theta_{ab}^v \leq \epsilon/r_{ab}(t)$ . We can then write the expression for



$\varkappa_{ab}(t, \tau)$  as

$$\varkappa_{ab}(t, \tau) = \Theta(\theta_{ab}^v \leq \epsilon/r_{ab}(t)) \int_0^\tau \delta(s - r_{ab}(t)/v_{ab}) ds, \quad (\text{B4})$$

which determines if a pair has collided given the relative location and velocities.

To derive the statistical properties of  $\varkappa_{ab}$ , we first average over the pair velocities. We assume a Maxwell-Boltzmann distribution for the velocity  $\mathbf{v}$ :

$$f(\mathbf{v})d^3\mathbf{v} = \pi^{-\frac{3}{2}} \frac{v^2}{v_T^3} e^{-v^2/v_T^2} dv \sin\theta_v d\theta_v d\varphi_v, \quad (\text{B5})$$

where  $v_T$  stands for the thermal relative velocity of the pair. The velocity-average collision probability is then given by

$$\begin{aligned} \langle \varkappa_{ab}(t, \tau) \rangle_v &\equiv \int \varkappa_{ab}(t, \tau) f(\mathbf{v}) d^3\mathbf{v} \\ &= \frac{\epsilon^2}{r_{ab}^2(t)} \frac{1}{\sqrt{\pi}} \int_{r_{ab}/\tau v_T}^\infty du u^2 e^{-u^2}, \end{aligned} \quad (\text{B6})$$

where we changed the integration variable to  $u = r_{ab}(t)/sv_T$ . The last integral can be approximated with using the Heaviside function,

$$\frac{1}{\sqrt{\pi}} \int_{r_{ab}/\tau v_T}^\infty du u^2 e^{-u^2} \approx \frac{1}{4} \Theta(\tau v_T - r_{ab}(t)), \quad (\text{B7})$$

yielding

$$\langle \varkappa_{ab}(t, \tau) \rangle_v \approx \frac{\sigma}{4\pi r_{ab}^2(t)} \Theta(\tau v_T - r_{ab}(t)), \quad (\text{B8})$$

such that two particles collide, on average, depending on their relative solid angle  $\sigma/4\pi r_{ab}^2(t)$ , provided that their spatial separation is small,  $r_{ab} < \tau v_T$ . Our model relies on the motion of the particles being ballistic, which is valid for short intervals  $v_T \tau \ll 1/n_B \sigma$ .

We are interested in the spatially coarse-grained dynamics on the length scale  $l \gg 1/n_B \sigma$ . Using the radial window function  $w(\mathbf{r})$ , we obtain

$$\begin{aligned} \langle \varkappa_{ab}(t, \tau) \rangle_v * w(\mathbf{r}) &= \frac{3}{4\pi l^3} \int_0^{2\pi} d\phi' \int_0^\pi \sin\theta' d\theta' \int_0^\infty r'^2 dr' \frac{\sigma}{4\pi r'^2} \Theta(\tau v_T - r') \Theta(|\mathbf{r}_{ab} - \mathbf{r}'| - l) \\ &\approx \frac{3}{4\pi l^3} \sigma \tau v_T \int_0^{2\pi} d\phi' \int_0^\pi \sin\theta' d\theta' \int_0^\infty r'^2 dr' \frac{\delta(r')}{4\pi r'^2} \Theta(|\mathbf{r}_{ab} - \mathbf{r}'| - l) = \frac{3}{4\pi l^3} \sigma \tau v_T \Theta(r_{ab} - l) \\ &= \sigma \tau v_T w(r_{ab}), \end{aligned} \quad (\text{B9})$$

where in the second line we used  $v_T \tau \ll l$ . This expression can be used to estimate standard kinematic relations, such as the mean collision times. The probability that two spins  $a$  and  $b$  will collide in time interval  $\tau$  is given by  $p_{ab}(t, \tau) = \langle \varkappa_{ab}(t, \tau) \rangle_v * w(\mathbf{r})$ . This probability is given by

$$p_a(t, \tau) = \sum_b p_{ab}(t, \tau) = \tau n_B \sigma v, \quad (\text{B10})$$

using the relation  $n_B = \sum_b w(\mathbf{r} - \mathbf{r}_b)$ . Since  $\tau_d^{(B)} \equiv 1/n_B \sigma v$  is the mean time between collisions for a given alkali-metal atom with any noble-gas atom, the probability is simply  $p_a = \tau/\tau_d^{(B)}$ , independent of  $t$ . This result corresponds to the Markovian exponential distribution  $p_a(t, \tau) = 1 - \exp(-\tau/\tau_d^{(B)})$  for  $\tau \ll \tau_d^{(B)}$ . A similar result is obtained for  $p_b(t, \tau)$  by interchanging the indices  $a$  and  $b$ .

We calculate the second moment of  $\varkappa_{ab}$  assuming that different collisions are statistically independent,

$$\langle \varkappa_{ab}(t, \tau) \varkappa_{cd}(t', \tau) \rangle_v = \delta_{ac} \delta_{bd} \tau \delta(t - t') \langle \varkappa_{ab}(t, \tau) \rangle_v, \quad (\text{B11})$$

where we assumed that the times  $t$  and  $t'$  are sampled with intervals  $dt, dt' \gg \tau$  to include multiple collisions.

Spin-exchange interactions, experienced during binary collisions as considered so far, lead to phase accumulation of the colliding spins. The spin dynamics are determined by the statistics of the collisions and are governed by

$$\varkappa_{ab}(t, \tau) \phi_{ab}(t) = \int_t^{t+\tau} \phi_{ab}^{(i)} \delta(s - t_{ab}^{(i)}) ds. \quad (\text{B12})$$

Since  $\varkappa_{ab}(t, \tau)$  is a Bernoulli process, whose possible values are only 0 or 1, we get

$$\langle \varkappa_{ab}(t, \tau) \phi_{ab}(t) \rangle = \langle \varkappa_{ab}(t, \tau) \rangle \langle \phi_{ab}(t) | \varkappa_{ab}(t, \tau) = 1 \rangle.$$

Moreover,  $\varkappa_{ab}(t, \tau)$  is defined such that when the spins  $a$  and  $b$  do not approach each other more closely than the collision distance  $\epsilon$ , then  $\phi_{ab}(t) = 0$ , and  $\phi_{ab}(t) \neq 0$  only when  $\varkappa_{ab}(t, \tau) = 1$ . Therefore,  $\langle \phi_{ab}(t) | \varkappa_{ab}(t, \tau) = 1 \rangle = \langle \phi_{ab}(t) \rangle = \langle \phi \rangle$ , where  $\langle \phi \rangle$  is averaged over all impact velocities and impact parameters. The value of  $\langle \phi \rangle$  and the dependence of  $\phi_{ab}(t)$  on the collision trajectory (velocity and impact parameter) were discussed in [37]. The averaged coupling strength is given by

$$\langle \varkappa_{ab}(t, \tau) \phi_{ab}(t) \rangle = \langle \phi \rangle \sigma v_T \tau w(r_{ab}). \quad (\text{B13})$$

Similarly, the averaged dissipation rate is given by

$$\langle \varkappa_{ab}(t, \tau) \phi_{ab}^2(t) \rangle = \langle \phi^2 \rangle \sigma v_T \tau w(r_{ab}), \quad (\text{B14})$$

and the fluctuation in second order is given by

$$\begin{aligned} & \langle \varkappa_{ab}(t, \tau) \phi_{ab}(t) \varkappa_{cd}(t', \tau) \phi_{cd}(t') \rangle \\ &= \delta_{ac} \delta_{bd} \sigma v_T w(r_{ab}) \langle \phi^2 \rangle \tau^2 \delta(t - t'). \end{aligned} \quad (\text{B15})$$

Equations (B9) and (B13) are used to derive the properties of  $\zeta$  in Eq. (21) as well as the identity in Eq. (C2). Equations (B11), (B14), and (B15) are used in deriving the properties of the incoherent exchange terms in Eq. (21) and in the derivation of the variance identities of the spin-exchange noise in Appendix C.

### APPENDIX C: NOISE ASSOCIATED WITH SPIN-EXCHANGE COLLISIONS

The fluctuation vector operator  $\hat{\mathbf{F}}_{\text{ex}}$  in Eq. (21) can be defined by (see Ref. [67])

$$\begin{aligned} \hat{\mathbf{F}}_{\text{ex}}(\mathbf{r}, t) dt &= -\zeta \hat{\mathbf{k}}(\mathbf{r}, t) \times \hat{\mathbf{f}}(\mathbf{r}, t) dt \\ &+ \frac{1}{\tau'} \int_t^{t+dt} ds \sum_{ab} \varkappa_{ab}(s, \tau') \phi_a(s) \\ &\times w(\mathbf{r}_b - \mathbf{r}_a) \hat{\mathbf{k}}_b \hat{\mathbf{s}}_a, \end{aligned} \quad (\text{C1})$$

accounting for the stochastic fine-grained dynamics [of Eq. (17)] within the coarse-grained description [of Eq. (21)]. Similarly to what we observe in the simulation in Sec. III and Fig. 2, the operator  $\hat{\mathbf{F}}_{\text{ex}}$  describes fluctuations of order  $\langle \phi^2 \rangle$  in the coherent mutual-precession process, manifesting a stochastic superposition of nonsymmetric local spin operators. Fluctuations in the incoherent terms are of order  $\langle \phi^4 \rangle$  and are thus negligible.

We now examine the statistical properties of the fluctuation operator  $\hat{\mathbf{F}}_{\text{ex}}$ . It is zero on average

$$\langle \hat{\mathbf{F}}_{\text{ex}}(\mathbf{r}, t) \rangle = 0, \quad (\text{C2})$$

and its correlations satisfy

$$\langle \hat{F}_{\text{ex},i}(\mathbf{r}, t) \hat{F}_{\text{ex},j}(\mathbf{r}', t') \rangle = \frac{1}{2} n_A n_B k_{\text{SE}} \delta(t - t') w(\mathbf{r} - \mathbf{r}') \hat{L}_{ij}, \quad (\text{C3})$$

where

$$\hat{L}_{ij} = \delta_{ij} \mathbb{1} - 2\{\hat{k}_i, \hat{s}_j\} / (n_A n_B) + i \epsilon_{ijm} (\hat{k}_m / n_B + \hat{s}_m / n_A). \quad (\text{C4})$$

Here the symbol  $\epsilon_{ijm}$  is the Levi-Civita tensor and  $i, j, m \in \{x, y, z\}$ . We interpret  $\hat{\mathbf{F}}_{\text{ex}}$  as temporally and spatially white, since its correlations are proportional to  $\delta(t - t')$  and to the coarse-grained  $\delta$  function  $w(\mathbf{r} - \mathbf{r}')$ . Furthermore, the coarse-grained commutation relations  $[\hat{s}_i(\mathbf{r}, t), \hat{s}_j(\mathbf{r}', t)] = i w(\mathbf{r} - \mathbf{r}') \epsilon_{ijm} \hat{s}_m(\mathbf{r}, t)$  and  $[\hat{k}_i(\mathbf{r}, t), \hat{k}_j(\mathbf{r}', t)] = i w(\mathbf{r} - \mathbf{r}') \epsilon_{ijm} \hat{k}_m(\mathbf{r}, t)$  are preserved. Indeed, the relaxation of the commutation relations after  $dt$  due to the loss terms in Eq. (21) is exactly balanced by the fluctuations  $\hat{F}_{\text{ex},i}(\mathbf{r}, t) \hat{F}_{\text{ex},j}(\mathbf{r}', t) dt^2$ . We therefore formally identify  $\hat{\mathbf{F}}_{\text{ex}}$  as a quantum white noise operator [42] originating from the randomness of the collisional interaction.

For fully polarized spin ensembles, the corresponding noise correlations are found to have the standard form of vacuum noise [42], satisfying

$$\begin{aligned} \langle \hat{F}_{\text{ex}}^-(\mathbf{r}, t) \hat{F}_{\text{ex}}^+(\mathbf{r}', t') \rangle &= 2 n_A n_B k_{\text{SE}} \delta(t - t') w(\mathbf{r} - \mathbf{r}'), \\ \langle \hat{F}_{\text{ex}}^+(\mathbf{r}, t) \hat{F}_{\text{ex}}^-(\mathbf{r}', t') \rangle &= 0. \end{aligned} \quad (\text{C5})$$

The contribution of  $\hat{\mathbf{F}}_{\text{ex}}$  to the alkali noise operator  $\hat{F}_A$  in Eqs. (25) and (28) is given by  $\hat{F}_A = \hat{F}_{\text{ex}}^- / \sqrt{2|f_z|}$ . Therefore, the variance is  $\langle \hat{F}_A(\mathbf{r}, t) \hat{F}_A^\dagger(\mathbf{r}', t') \rangle = 2 \gamma_{\text{ex}} \delta(t - t') w(\mathbf{r} - \mathbf{r}')$ , where  $\gamma_{\text{ex}} = n_B k_{\text{SE}} / q$  is the spin-exchange relaxation for the alkali spins. We thus conclude that, for polarized ensembles, the spin-exchange noise appears as vacuum noise, which is the minimal possible noise.

It is also interesting to consider the case of imperfect spin polarization. For general spin polarizations  $p_A, p_B \leq 1$ , the second-order moments of the noise are given by

$$\begin{aligned} \langle \hat{F}_A(\mathbf{r}, t) \hat{F}_A^\dagger(\mathbf{r}', t') \rangle &= \frac{2 + p_A + p_B}{4 p_A} 2 \gamma_{\text{ex}} \delta(t - t') w(\mathbf{r} - \mathbf{r}'), \\ \langle \hat{F}_A^\dagger(\mathbf{r}, t) \hat{F}_A(\mathbf{r}', t') \rangle &= \frac{2 - p_A - p_B}{4 p_A} 2 \gamma_{\text{ex}} \delta(t - t') w(\mathbf{r} - \mathbf{r}'). \end{aligned}$$

Importantly, for highly polarized ensembles ( $1 - p_A \ll 1$ ,  $1 - p_B \ll 1$ ), the excess noise is small, since

$(2 - p_A - p_B/4p_A) \ll 1$  and  $(2 + p_A + p_B/4p_A) - 1 \ll 1$ . It is interesting to note that imperfect polarization contributes to other quantum noise terms as well, and this contribution is quantitatively similar to that in  $\hat{\mathbf{F}}_{\text{ex}}$  and  $\hat{F}_A$ . We therefore conclude that the interface based on spin-exchange collisions is not much more sensitive to imperfect polarization compared with other quantum effects in single-species spin systems.

In practice, the relaxation due to spin exchange, including the effect of  $\hat{\mathbf{F}}_{\text{ex}}$ , is small compared with that originating from other sources. For example, the relaxation rate of the alkali electron spin due to spin exchange is  $n_B k_{\text{SE}}$ , whereas the relaxation rate due to the spin-rotation coupling during collisions is  $n_B \sigma_{\text{SR}} v$ , where  $\sigma_{\text{SR}}$  is the spin-rotation cross section. The relative importance of these two mechanisms is characterized by the parameter  $\eta = k_{\text{SE}}/\sigma_{\text{SR}} v$ , where  $\eta = 0.34$  for potassium-helium,  $\eta = 0.024$  for rubidium-helium, and  $\eta < 0.01$  for cesium-helium at 215 °C [11]. The relaxation of the noble-gas spins due to spin exchange with alkali spins is negligible for  $t \ll (n_A k_{\text{SE}})^{-1} \approx 17$  h when one is operating with  $n_A = 3 \times 10^{14}$  cm<sup>-3</sup>. When perfectly polarized ensembles are initialized, quantum noises other than spin exchange also behave as vacuum noises. In this case, the noise terms  $\hat{F}_A = (\hat{F}_{A,x} + i\hat{F}_{A,y})/\sqrt{2|f_z|}$  and  $\hat{F}_B = (\hat{F}_{B,x} + i\hat{F}_{B,y})/\sqrt{2|k_z|}$  satisfy

$$\langle \hat{F}_\chi \rangle = \langle \hat{F}_\chi^\dagger \hat{F}_\chi \rangle = 0 \quad (\text{C6})$$

and

$$\begin{aligned} \langle \hat{F}_\chi(\mathbf{r}, t), \hat{F}_\chi^\dagger(\mathbf{r}', t') \rangle &= \langle \hat{F}_\chi(\mathbf{r}, t) \hat{F}_\chi^\dagger(\mathbf{r}', t') \rangle \\ &= [2\gamma_\chi w(\mathbf{r} - \mathbf{r}') + C_\chi(\mathbf{r}, \mathbf{r}')] \delta(t - t'), \end{aligned} \quad (\text{C7})$$

for  $\chi \in \{A, B\}$ , including the fluctuations induced by the spin-exchange interaction. The function  $C_\chi(\mathbf{r}, \mathbf{r}')$  is the diffusion component of the noise correlation function [40], independent of the spin-exchange interaction or of the other relaxation mechanisms incorporated in  $\gamma_\chi$ .

Partially polarized ensembles exhibit increased quantum noise. An ensemble with polarization  $p_\chi = 1 - \delta p_\chi$  for  $\delta p_\chi \ll 1$ , is populated with incoherent (thermal) excitations of each spin mode by  $\langle \hat{n}_l \rangle = (1 - p)/2p \approx \delta p/2$ . Thus, the noise variance exceeds that of vacuum noise and is given by

$$\begin{aligned} \langle \hat{F}_\chi^\dagger(\mathbf{r}, t) \hat{F}_\chi(\mathbf{r}', t') \rangle &= \delta p_\chi / 2 [2\gamma_\chi w(\mathbf{r} - \mathbf{r}') \\ &+ C_\chi(\mathbf{r}, \mathbf{r}')] \delta(t - t') \end{aligned} \quad (\text{C8})$$

and

$$\begin{aligned} \langle \hat{F}_\chi(\mathbf{r}, t) \hat{F}_\chi^\dagger(\mathbf{r}', t') \rangle &= (1 + \delta p_\chi / 2) [2\gamma_\chi w(\mathbf{r} - \mathbf{r}') \\ &+ C_\chi(\mathbf{r}, \mathbf{r}')] \delta(t - t'). \end{aligned} \quad (\text{C9})$$

## APPENDIX D: COMPARISON WITH MEAN-FIELD MODEL.

We compare Eq. (21) with the existing mean-field theory and associate our model parameters with those obtained from experiments. The mean-field spin operators are related to our formalism by  $\langle \hat{\mathbf{f}} \rangle \equiv \int d^3r \langle \psi | \hat{\mathbf{f}}(\mathbf{r}, t) | \psi \rangle / N_A$  and  $\langle \hat{\mathbf{k}} \rangle \equiv \int d^3r \langle \psi | \hat{\mathbf{k}}(\mathbf{r}, t) | \psi \rangle / N_B$ , where  $|\psi\rangle$  is the initial many-body wave function of the system. Substituting these definitions in Eq. (21) and using  $\langle \hat{\mathbf{F}}_{\text{ex}} \rangle = 0$ , we recover the standard Bloch equations [Eq. (1)].

In terms of experimentally measured parameters, the interaction strength  $\zeta$  is given by  $\zeta = 8\pi\kappa_0 g_e g_n \mu_B \mu_n / 3q\hbar$ , where  $g_e = 2$  is the electron  $g$  factor,  $g_n$  is the  $g$  factor of the noble-gas nucleus,  $\mu_B$  is the Bohr magneton,  $\mu_n$  is the magnetic moment of the noble-gas spin, and  $\kappa_0$  is the enhancement factor over the classical magnetic field due to the attraction of the alkali-metal electron with the noble-gas nucleus during a collision [11,38]. For K-<sup>3</sup>He at  $T = 220$  °C,  $\zeta = 4.9 \times 10^{-15}$  cm<sup>3</sup>/s, and  $k_{\text{SE}} = 5.5 \times 10^{-20}$  cm<sup>3</sup>/s [11,38]. Roughly estimating a collisional spin-exchange cross section  $\sigma$  of approximately  $8 \times 10^{-15}$  cm<sup>2</sup> from the K-<sup>3</sup>He interatomic potential [68] and using a typical centrifugal potential with an angular momentum of  $40\hbar$  yields an estimate of the precession angles  $\langle \phi \rangle \approx \zeta q / \sigma v = 1.4 \times 10^{-5}$  rad and  $\langle \phi^2 \rangle \approx 4k_{\text{SE}} / \sigma v = 1.6 \times 10^{-10}$  rad<sup>2</sup> for highly polarized alkali vapor.

## APPENDIX E: COUPLED SPATIAL MODES

The expressions in Eq. (27) describe the coupling of any spatial mode of one spin species with the  $N_{\text{modes}} \approx V/V_l$  modes of the other species. In practice, however, most modes are barely coupled. It is constructive to differentiate between the set of high-order modes of the diffusion operator, defined by  $\mathcal{R} \equiv \{\hat{a}_r, \hat{b}_r | \gamma_{Ar}, \gamma_{Br} \gg J\}$  ( $0 \leq r < N_{\text{modes}}$ ) and the complementary set of stable modes,  $\mathcal{S} = 1 \setminus \mathcal{R}$ . The high-order modes,  $\mathcal{R}$ , are characterized by rapid relaxation due to the thermal motion of the atoms. These modes experience little coherent interaction and, at long timescales  $dt \gg 1/\gamma_{Ar}, 1/\gamma_{Br}$ , are governed by

$$\begin{aligned} \hat{a}_r(t) &= \hat{w}_{Ar}(t) - \frac{iJ}{\gamma_{Ar} - i\Delta} \sum_{n \in \mathcal{S}} c_{rn} \hat{b}_n(t), \\ \hat{b}_r(t) &= \hat{w}_{Br}(t) - \frac{iJ}{\gamma_{Br} + i\Delta} \sum_{m \in \mathcal{S}} c_{mr}^* \hat{a}_m(t). \end{aligned} \quad (\text{E1})$$

The first terms,  $\hat{w}_{\chi r}(t) = \int_0^t d\tau' e^{-(i\omega_\chi + \gamma_{\chi r})\tau'} \hat{F}_{\chi r}(t - \tau')$  for  $\chi \in \{A, B\}$ , describe the diffusion-induced quantum process. Here we used the noise terms of the  $r$ th modes, which are given by  $\hat{F}_{Ar} = \int A_r(\mathbf{r}) \hat{F}_A(\mathbf{r}) d^3\mathbf{r}$  and  $\hat{F}_{Br} = \int B_r(\mathbf{r}) \hat{F}_B(\mathbf{r}) d^3\mathbf{r}$ . This process dominates the dynamics, which is Markovian: any dependence on  $\hat{a}_r(t_0)$  and  $\hat{b}_r(t_0)$  at  $t_0 \ll t$  is erased exponentially at the fast rates  $\gamma_{Ar}$  and  $\gamma_{Br}$ . Consequently, the modes  $\hat{a}_r(t)$  and  $\hat{b}_r(t)$  can be considered

as thermal reservoirs. The second term in the expressions in Eq. (E1) describes the weak coupling to the stable modes  $\hat{a}_s, \hat{b}_s \in \mathcal{S}$  via the coherent collisional interaction. Substitution of the expressions in Eq. (E1) in the expressions in Eq. (27) yields a relatively small and close set of coupled equations for the stable modes, governed by a coherent dynamics:

$$\begin{aligned}\partial_t \hat{a}_s &= -(i\omega_A + \gamma_{As})\hat{a}_s - J \sum_{n \in \mathcal{S}} (ic_{sn}\hat{b}_n + \epsilon_{sn}^{(A)}\hat{a}_n) + \hat{G}_{As}, \\ \partial_t \hat{b}_s &= -(i\omega_B + \gamma_{Bs})\hat{b}_s - J \sum_{m \in \mathcal{S}} (ic_{ms}^*\hat{a}_m + \epsilon_{sm}^{(B)*}\hat{b}_m) + \hat{G}_{Bs},\end{aligned}\quad (\text{E2})$$

The coefficients  $\epsilon_{sn}^{(A)} = \sum_{r \in \mathcal{R}} c_{sr}c_{nr}^*J/(\gamma_{Br} + i\Delta)$  and  $\epsilon_{sn}^{(B)} = \sum_{r \in \mathcal{R}} c_{rs}c_{rn}^*J/(\gamma_{Ar} - i\Delta)$  describe couplings between different stable modes, and  $\hat{G}_{As} = \hat{F}_{As} - iJ \sum_{r \in \mathcal{R}} c_{sr}\hat{w}_{Br}$  and  $\hat{G}_{Bs} = \hat{F}_{Bs} - iJ \sum_{r \in \mathcal{R}} c_{rs}\hat{w}_{Ar}$  denote the increased quantum noise induced due to coupling with the high-order (reservoir) modes,  $\mathcal{R}$ .

The effect of  $\hat{G}_{As}$  and  $\hat{G}_{Bs}$  on the spin dynamics depends on the number of modes considered in  $\mathcal{S}$ . For the case of an uncoated spherical cell with radius  $R$ , we can bound the contribution of the high-order modes by  $|\epsilon_{sn}^{(A/B)}| < J/\pi^2\gamma_{(B/A)r_0}$ . Here  $\gamma_{(B/A)r_0} = D_{(B/A)}\pi^2r_0^2/R^2$  is the diffusion-induced relaxation of the least-decaying mode in the set  $\mathcal{R}$ , with radial mode number  $r_0$ . This bound is attained by the asymptotic form of the diffusion-relaxation modes, validated by numerical calculations. Thus, if enough modes are considered in Eq. (E2), the contributions of  $\epsilon_{sn}^{(A)}$ ,  $\epsilon_{sn}^{(B)}$ ,  $\hat{G}_A - \hat{F}_A$ , and  $\hat{G}_B - \hat{F}_B$  to the dynamics can be rendered negligible. In general, this formalism can also be applied with a smaller number of stable modes such that  $\gamma_{Am}, \gamma_{Bn} \sim J$ , at the expense of overestimating the diffusion-induced relaxation. Moreover, one may calculate  $\epsilon_{sn}^{(A)}$  and  $\epsilon_{sn}^{(B)}$  for a given number of leading reservoir modes and use the asymptotic approximation for the infinite number of additional reservoir modes; namely,  $\epsilon_{sn}^{(A)} = \sum_{r=r_0}^{r_1} c_{sr}c_{nr}^*J/(\gamma_{Br} + i\Delta) + J/\pi^2\gamma_{Br_1}$  and  $\epsilon_{sn}^{(B)} = \sum_{r=r_1}^{r_h-1} Jc_{rs}c_{rn}^*/(\gamma_{Ar} - i\Delta) + J/\pi^2\gamma_{Ar_h}$ .

## APPENDIX F: TWO-MODE SOLUTION

Here we consider the analytical solution of Eqs. (28a) and (28b). These equations describe a simplified model with only a single mode per spin species (the stable mode  $s = 0$ , with  $c_{00} = 1$ ). For  $\Delta = 0$ , the dynamics are given by

$$\begin{aligned}\hat{a}(t) &= e^{-\frac{\gamma t}{2}} \left[ \left( \cos \tilde{J}t - \frac{\gamma}{2\tilde{J}} \sin \tilde{J}t \right) \hat{a} - \frac{iJ}{\tilde{J}} \sin(\tilde{J}t) \hat{b} \right] + \hat{w}_A, \\ \hat{b}(t) &= e^{-\frac{\gamma t}{2}} \left[ \left( \cos \tilde{J}t + \frac{\gamma}{2\tilde{J}} \sin \tilde{J}t \right) \hat{b} - \frac{iJ}{\tilde{J}} \sin(\tilde{J}t) \hat{a} \right] + \hat{w}_B,\end{aligned}$$

where the effective exchange rate is given by

$$\tilde{J} = \sqrt{J^2 - \gamma^2/4} \quad (\text{F1})$$

and the quantum noise processes are

$$\begin{aligned}\hat{w}_A(t) &= \int_0^t ds e^{-\gamma s/2} \left( \cos \tilde{J}s - \frac{\gamma}{2\tilde{J}} \sin \tilde{J}s \right) \hat{F}_A(t-s), \\ \hat{w}_B(t) &= -i \int_0^t ds e^{-\gamma s/2} \frac{J}{\tilde{J}} \sin(\tilde{J}s) \hat{F}_A(t-s).\end{aligned}\quad (\text{F2})$$

In the strong-coupling regime  $J \gg \gamma$ , the full solution in the rotating frame further simplifies to

$$\begin{aligned}\hat{a}(t) &= e^{-\gamma t/2} [\cos(Jt)\hat{a} - i \sin(Jt)\hat{b}] + \hat{w}_A, \\ \hat{b}(t) &= e^{-\gamma t/2} [\cos(Jt)\hat{b} - i \sin(Jt)\hat{a}] + \hat{w}_B.\end{aligned}\quad (\text{F3})$$

Here the alkali-metal relaxation is shared by both spin gases, accompanied by a transfer of quantum fluctuations to the noble-gas spin. The noise processes simplify to

$$\begin{aligned}\hat{w}_A(t) &= \int_0^t ds e^{-\gamma s/2} \cos(Js) \hat{F}_A(t-s), \\ \hat{w}_B(t) &= -i \int_0^t ds e^{-\gamma s/2} \sin(Js) \hat{F}_A(t-s).\end{aligned}\quad (\text{F4})$$

For  $t \gg 2/\gamma$ , these processes can be considered as white Wiener operators, while for shorter times, they are colored by the transfer functions. It is fruitful to derive the explicit noise statistics of  $\hat{w}_B$  in the strong-coupling regime with respect to the vacuum state. The noise process has zero average  $\langle \hat{w}_B(t) \rangle = 0$ , and the other moments satisfy  $\langle \hat{w}_B(t) \hat{w}_B(t') \rangle = \langle \hat{w}_B^\dagger(t) \hat{w}_B(t') \rangle = 0$ . However, this process has a nonzero correlation

$$\langle \hat{w}_B(t) \hat{w}_B^\dagger(t') \rangle = 2\gamma e^{-\frac{\gamma|t-t'|}{2}} \int_0^t ds e^{-\gamma s} \sin(Js) \sin(Js')$$

using  $\langle \hat{F}_A(t) \hat{F}_A^\dagger(t') \rangle = 2\gamma \delta(t-t')$  and denoting  $s' = s + |t-t'|$ . It is also interesting to look at  $t = t'$ , which, up to first order in  $\gamma/J$ , is given by

$$\langle \hat{w}_B(t) \hat{w}_B^\dagger(t) \rangle = 1 - e^{-\gamma t} \left( 1 + \frac{\gamma}{2J} \sin 2Jt \right), \quad (\text{F5})$$

thus vanishing at  $t = 0$  and approaching unity for  $t \gg \gamma^{-1}$ . At the exchange time  $T_\pi$ , it is given by

$$\langle \hat{w}_B(T_\pi) \hat{w}_B^\dagger(T_\pi) \rangle = \frac{\gamma\pi}{2J} \quad (\text{F6})$$

to first order in  $\gamma/J$ .

We now consider the exchange of spin-squeezed states. Substituting the expressions in Eq. (F3) in Eq. (36), we find that the evolution for  $\gamma = 0$  is given by

$$|\psi(t)\rangle = \exp \left\{ \frac{1}{2} \left[ \cos^2(Jt) (\xi^* a^2 - \xi a^{\dagger 2}) - \sin^2(Jt) (\xi^* b^2 - \xi b^{\dagger 2}) - i \sin(2Jt) (\xi^* ab + \xi a^\dagger b^\dagger) \right] \right\} |0\rangle_A |0\rangle_B. \quad (\text{F7})$$

We find that the noble gas is squeezed at  $T_\pi$  and that, at intermediate times, the spins of the two gases become entangled.

In the presence of relaxation and noise, the system does not remain in a pure spin-squeezed state after the exchange due to excitations of nonsymmetric spin modes. Yet, as we now show, it retains a spin variance below the standard quantum limit in the  $\hat{P}_B$  quadrature. The evolution of  $\hat{X}_B(t)$  and that of  $\hat{P}_B(t)$  are given by

$$\begin{aligned} \hat{X}_B(t) &= e^{-\gamma t} \left[ \cos(Jt) \hat{X}_B + \sin(Jt) \hat{P}_A \right] + \hat{w}_{X_B}(t), \\ \hat{P}_B(t) &= e^{-\gamma t} \left[ \cos(Jt) \hat{P}_B - \sin(Jt) \hat{X}_A \right] + \hat{w}_{P_B}(t), \end{aligned} \quad (\text{F8})$$

where  $\hat{w}_{X_B} = (\hat{w}_B + \hat{w}_B^\dagger)/2$  and  $\hat{w}_{P_B} = i(\hat{w}_B^\dagger - \hat{w}_B)/2$  are Hermitian noise processes, whose vacuum statistics satisfy

$$\langle \hat{w}_{X_B}^2 \rangle = \langle \hat{w}_{P_B}^2 \rangle = \langle \hat{w}_B(t) \hat{w}_B^\dagger(t) \rangle / 4. \quad (\text{F9})$$

To compute the variance of spin-squeezed states, it is fruitful to define the spin-squeezing operator

$$\hat{S}(\hat{a}, \xi) = \exp \left[ \frac{1}{2} (\xi^* \hat{a}^2 - \xi \hat{a}^{\dagger 2}) \right], \quad (\text{F10})$$

for which  $|\xi\rangle_A = \hat{S}(\hat{a}, \xi)|0\rangle_A$ , and which for  $\xi = |\xi|e^{i\theta}$  satisfies

$$\hat{S}^\dagger(\hat{a}, \xi) \hat{a} \hat{S}(\hat{a}, \xi) = \cosh(|\xi|) \hat{a} - e^{i\theta} \sinh(|\xi|) \hat{a}^\dagger. \quad (\text{F11})$$

Using Eqs. (F8) and (F11), we find that the exchanged variances are given by

$$\begin{aligned} \Delta \hat{X}_B^2(t) &= e^{-\gamma t} \left[ \cos^2(Jt) \langle \hat{X}_B^2 \rangle + \sin^2(Jt) \langle \hat{P}_A^2 \rangle \right] + \langle \hat{w}_{X_B}^2(t) \rangle, \\ \Delta \hat{P}_B^2(t) &= e^{-\gamma t} \left[ \cos^2(Jt) \langle \hat{P}_B^2 \rangle + \sin^2(Jt) \langle \hat{X}_A^2 \rangle \right] + \langle \hat{w}_{P_B}^2(t) \rangle, \end{aligned} \quad (\text{F12})$$

where the expectation values are taken for  $|\psi(0)\rangle$ . Using  $t = T_\pi$ , we then obtain Eq. (38).

## APPENDIX G: MAGNETOMETER RESPONSE

To describe the response of the hybrid alkali–noble-gas magnetometer, we extend the simplified two-mode model in Eq. (28) to include a time-varying transverse magnetic field and a nonzero noble-gas relaxation:

$$\begin{pmatrix} \partial_t \hat{a} \\ \partial_t \hat{b} \end{pmatrix} = \begin{pmatrix} i\omega_A - \gamma_A & -iJ \\ -iJ & i\omega_B - \gamma_B \end{pmatrix} \begin{pmatrix} \hat{a} \\ \hat{b} \end{pmatrix} + \begin{pmatrix} \hat{h}_A \\ \hat{h}_B \end{pmatrix}, \quad (\text{G1})$$

where the inhomogeneous source terms are

$$\begin{aligned} \hat{h}_A &= \hat{F}_A + iB_\perp g_A \sqrt{qN_A p_A} / 2, \\ \hat{h}_B &= \hat{F}_B + iB_\perp g_B \sqrt{N_B p_B} / 2. \end{aligned} \quad (\text{G2})$$

The time evolution of  $\hat{a}(t)$  is obtained by integration of Eq. (G1), which yields

$$\begin{aligned} \hat{a}(t) &= \Phi_{(t,0)}^A \hat{a} + \Phi_{(t,0)}^B \hat{b} \\ &+ \int_0^t \left( \Phi_{(t,\tau)}^A \hat{h}_A(\tau) + \Phi_{(t,\tau)}^B \hat{h}_B(\tau) \right) d\tau. \end{aligned} \quad (\text{G3})$$

Here  $\Phi_{(t,\tau)}^A$  and  $\Phi_{(t,\tau)}^B$  are the transfer functions of the operator  $\hat{a}(t)$  to excitations of  $\hat{a}(\tau)$  and  $\hat{b}(\tau)$  at an earlier time  $\tau$ , respectively, which are given by exponentiation of the homogeneous part of Eq. (G1):

$$\Phi_{(t,\tau)}^A = \frac{1}{2i\tilde{J}} \left( \Lambda_+ e^{\Pi_+(t-\tau)} + \Lambda_- e^{\Pi_-(t-\tau)} \right) \quad (\text{G4})$$

and

$$\Phi_{(t,\tau)}^B = \frac{J}{2\tilde{J}} \left( e^{\Pi_-(t-\tau)} - e^{\Pi_+(t-\tau)} \right). \quad (\text{G5})$$

The coupling rate

$$\tilde{J} = \sqrt{J^2 + \frac{1}{4}(\Delta + i\gamma_A - i\gamma_B)^2} \quad (\text{G6})$$

generalizes Eq. (F1) for nonzero detuning and noble-gas relaxation, and the dressed-state rates and amplitudes are given by

$$\Pi_\pm = \pm i\tilde{J} - \frac{1}{2}(\gamma_A + \gamma_B - i\omega_A - i\omega_B), \quad (\text{G7})$$

$$\Lambda_\pm = i\tilde{J} \pm \frac{1}{2}(i\Delta + \gamma_B - \gamma_A). \quad (\text{G8})$$

In the detuned limit considered in this analysis, the rates  $\Pi_\pm$  conveniently simplify to decoupled alkali and noble-gas dynamics

$$\Pi_+ = i\left(\omega_A + \frac{J^2}{\Delta}\right) - \gamma_A \left(1 - \frac{J^2}{\Delta^2}\right), \quad (\text{G9})$$

$$\Pi_- = i\left(\omega_B - \frac{J^2}{\Delta}\right) - \left(\gamma_B + \frac{J^2}{\Delta^2}\gamma_A\right) \equiv i\tilde{\omega}_B - \tilde{\gamma}_B \quad (\text{G10})$$

to leading orders in  $J/\Delta$ . Here  $\tilde{\omega}_B$  denotes the dressed precession frequency of the noble gas, and  $\tilde{\gamma}_B$  denotes the dressed relaxation rate. Similarly, the dressed amplitudes  $\Lambda_{\pm}$  are given by

$$\Lambda_+ = i\Delta + \gamma_B - \gamma_A, \quad (\text{G11})$$

$$\Lambda_- = i\frac{J^2}{\Delta} + \frac{J^2}{\Delta^2}\gamma_A. \quad (\text{G12})$$

We now turn to compute the terms composing  $M(T)$  in Eq. (40). We consider a transverse magnetic field  $B_{\perp} = B_x - iB_y$ , oscillating in resonance with the noble-gas precession  $\omega = \tilde{\omega}_B$  and apply the rotating-wave approximation under the assumptions that  $\omega_A \gg \gamma_A$  and  $\omega_B \gg \tilde{\gamma}_B$ . We find that the magnetometer signal is composed of three terms:

$$\hat{M} = \langle \hat{M} \rangle + \delta\hat{M}_{\text{init}} + \delta\hat{M}_F. \quad (\text{G13})$$

The first term describes the lock-in response to the magnetic signal, which is given by

$$|\langle \hat{M} \rangle| = \frac{Jg_B\sqrt{N_B P_B} \text{Re } B_{\perp}}{8\Delta\tilde{\gamma}_B^2 T} (1 + \varrho) \left( \tilde{\gamma}_B T + e^{-\tilde{\gamma}_B T} - 1 \right), \quad (\text{G14})$$

where

$$\varrho = \frac{g_A J}{g_B \Delta} \sqrt{\frac{q N_{AP_A}}{N_B P_B}} \quad (\text{G15})$$

denotes the relative response of the alkali spins to the driving field with respect that of the noble gas, and for simplicity we can assume that the noble-gas density is sufficiently high such that  $\varrho \ll 1$ . The second and third terms in Eq. (G13) denote the noise processes associated with atom projection noise, which fundamentally limit the sensitivity of the sensor. Both terms vanish on average ( $\langle \delta\hat{M}_{\text{init}} \rangle = \langle \delta\hat{M}_F \rangle = 0$ ) but have nonzero standard deviations. The first is given by

$$\sqrt{\langle \delta\hat{M}_{\text{init}}^2 \rangle} = \frac{J(1 - e^{-\tilde{\gamma}_B T})}{2\Delta\tilde{\gamma}_B T} \sqrt{\langle P_B^2 \rangle + \frac{J^2}{\Delta^2} \langle P_A^2 \rangle}, \quad (\text{G16})$$

which depends predominantly on the noble-gas initial spin variance and is significant for  $T \ll \tilde{\gamma}_B^{-1}$ . The second,

$$\sqrt{\langle \delta\hat{M}_F^2 \rangle} = \frac{J\sqrt{2\tilde{\gamma}_B T - 3 + 4e^{-\tilde{\gamma}_B T} - e^{-2\tilde{\gamma}_B T}}}{4\Delta\tilde{\gamma}_B T}, \quad (\text{G17})$$

is associated with relaxation and coupling of noise at rate  $\tilde{\gamma}_B$ , which becomes significant at later times. The magnetic

sensitivities are therefore limited by

$$\delta B_{\text{init}} = B_{\perp} \frac{\sqrt{\langle \delta\hat{M}_{\text{init}}^2 \rangle}}{|\langle \hat{M} \rangle|} \quad \text{and} \quad \delta B_F = B_{\perp} \frac{\sqrt{\langle \delta\hat{M}_F^2 \rangle}}{|\langle \hat{M} \rangle|}.$$

- 
- [1] B. Julsgaard, A. Kozhekin, and E. S. Polzik, Experimental long-lived entanglement of two macroscopic objects, *Nature (London)* **413**, 400 (2001), arXiv:quant-ph/0106057 [quant-ph].
  - [2] K. Hammerer, A. S. Sørensen, and E. S. Polzik, Quantum interface between light and atomic ensembles, *Rev. Mod. Phys.* **82**, 1041 (2010), arXiv:0807.3358 [quant-ph].
  - [3] J. F. Sherson, H. Krauter, R. K. Olsson, B. Julsgaard, K. Hammerer, I. Cirac, and E. S. Polzik, Quantum teleportation between light and matter, *Nature (London)* **443**, 557 (2006), arXiv:quant-ph/0605095 [quant-ph].
  - [4] D. F. Phillips, A. Fleischhauer, A. Mair, R. L. Walsworth, and M. D. Lukin, in *APS Division of Atomic, Molecular and Optical Physics Meeting Abstracts*, APS Meeting Abstracts, Vol. 46 (2001), p. Q4.010.
  - [5] M. Fleischhauer and M. D. Lukin, Dark-State Polaritons in Electromagnetically Induced Transparency, *Phys. Rev. Lett.* **84**, 5094 (2000), arXiv:quant-ph/0001094 [quant-ph].
  - [6] M. D. Eisaman, A. André, F. Massou, M. Fleischhauer, A. S. Zibrov, and M. D. Lukin, Electromagnetically induced transparency with tunable single-photon pulses, *Nature (London)* **438**, 837 (2005).
  - [7] M. Hosseini, G. Campbell, B. M. Sparkes, P. K. Lam, and B. C. Buchler, Unconditional room-temperature quantum memory, *Nat. Phys.* **7**, 794 (2011), arXiv:1412.8235 [quant-ph].
  - [8] R. Finkelstein, E. Poem, O. Michel, O. Lahad, and O. Firstenberg, Fast, noise-free memory for photon synchronization at room temperature, *Sci. Adv.* **4**, eaap8598 (2018), arXiv:1708.01919 [quant-ph].
  - [9] K. T. Kaczmarek, P. M. Ledingham, B. Brecht, S. E. Thomas, G. S. Thekkadath, O. Lazo-Arjona, J. H. D. Munns, E. Poem, A. Feizpour, D. J. Saunders, J. Nunn, and I. A. Walmsley, High-speed noise-free optical quantum memory, *Phys. Rev. A* **97**, 042316 (2018), arXiv:1704.00013 [quant-ph].
  - [10] F. Ripka, H. Kübler, R. Löw, and T. Pfau, A room-temperature single-photon source based on strongly interacting rydberg atoms, *Science* **362**, 446 (2018), arXiv:1806.02120 [physics.atom-ph].
  - [11] W. Happer, Y.-Y. Jau, and T. Walker, *Optically Pumped Atoms* (WILEY-VCH, Weinheim, Germany, 2010), ISBN 978-3-527-40707-1.
  - [12] D. Budker and D. F. J. Kimball, *Optical Magnetometry* (Cambridge University Press, Cambridge, England, 2013).
  - [13] M. V. Balabas, T. Karaulanov, M. P. Ledbetter, and D. Budker, Polarized Alkali-Metal Vapor with Minute-Long Transverse Spin-Relaxation Time, *Phys. Rev. Lett.* **105**, 070801 (2010).

- [14] O. Katz, O. Peleg, and O. Firstenberg, Coherent Coupling of Alkali Atoms by Random Collisions, *Phys. Rev. Lett.* **115**, 113003 (2015), arXiv:1505.02241 [physics.atom-ph].
- [15] G. Vasilakis, H. Shen, K. Jensen, M. Balabas, D. Salart, B. Chen, and E. S. Polzik, Generation of a squeezed state of an oscillator by stroboscopic back-action-evading measurement, *Nat. Phys.* **11**, 389 (2015), arXiv:1411.6289 [quant-ph].
- [16] H. Bao, J. Duan, S. Jin, X. Lu, P. Li, W. Qu, M. Wang, I. Novikova, E. E. Mikhailov, K.-F. Zhao, K. Mølmer, H. Shen, and Y. Xiao, Spin squeezing of 1011 atoms by prediction and retrodiction measurements, *Nature (London)* **581**, 159 (2020).
- [17] R. A. Thomas, M. Parniak, C. Østfeldt, C. B. Møller, C. Bærentsen, Y. Tsaturyan, A. Schliesser, J. Appel, E. Zeuthen, and E. S. Polzik, Entanglement between distant macroscopic mechanical and spin systems, *Nat. Phys.* **17**, 228 (2021), arXiv:2003.11310 [quant-ph].
- [18] J. Kong, R. Jiménez-Martínez, C. Troullinou, V. G. Lucivero, G. Toth, and M. W. Mitchell, Measurement-induced, spatially-extended entanglement in a hot, strongly-interacting atomic system, *Nat. Commun.* **11** (2020).
- [19] I. K. Kominis, Sub-Shot-Noise Magnetometry with a Correlated Spin-Relaxation Dominated Alkali-Metal Vapor, *Phys. Rev. Lett.* **100**, 073002 (2008), arXiv:0708.0330 [physics.atom-ph].
- [20] A. T. Dellis, M. Loulakis, and I. K. Kominis, Spin-noise correlations and spin-noise exchange driven by low-field spin-exchange collisions, *Phys. Rev. A* **90**, 032705 (2014), arXiv:1307.2596 [physics.atom-ph].
- [21] W. C. Chen, T. R. Gentile, C. B. Fu, S. Watson, G. L. Jones, J. W. McIver, and D. R. Rich, in *Journal of Physics Conference Series*, Journal of Physics Conference Series, Vol. 294 (2011), p. 012003.
- [22] C. Gemmel, W. Heil, S. Karpuk, K. Lenz, C. Ludwig, Y. Sobolev, K. Tullney, M. Burghoff, W. Kilian, S. Knappe-Grüneberg, W. Müller, A. Schnabel, F. Seifert, L. Trahms, and S. Baeßler, Ultra-sensitive magnetometry based on free precession of nuclear spins, *Eur. Phys. J. D* **57**, 303 (2010).
- [23] T. R. Gentile, P. J. Nacher, B. Saam, and T. G. Walker, Optically polarized  $^3\text{He}$ , *Rev. Mod. Phys.* **89**, 045004 (2017), arXiv:1612.04178 [physics.atom-ph].
- [24] W. Heil, C. Gemmel, S. Karpuk, Y. Sobolev, K. Tullney, F. Allmendinger, U. Schmidt, M. Burghoff, W. Kilian, S. Knappe-Grüneberg, A. Schnabel, F. Seifert, and L. Trahms, Spin clocks: Probing fundamental symmetries in nature, *Annalen der Physik* **525**, 539 (2013).
- [25] A. Dantan, G. Reinaudi, A. Sinatra, F. Laloë, E. Giacobino, and M. Pinard, Long-Lived Quantum Memory with Nuclear Atomic Spins, *Phys. Rev. Lett.* **95**, 123002 (2005), arXiv:quant-ph/0504152 [quant-ph].
- [26] G. Reinaudi, A. Sinatra, A. Dantan, and M. Pinard, Squeezing and entangling nuclear spins in helium 3, *J. Mod. Opt.* **54**, 675 (2007), arXiv:quant-ph/0512186 [quant-ph].
- [27] A. Serafin, M. Fadel, P. Treutlein, and A. Sinatra, arXiv e-prints, arXiv:2012.07216 (2020).
- [28] A. Serafin, Y. Castin, M. Fadel, P. Treutlein, and A. Sinatra, arXiv e-prints, arXiv:2012.14686 (2020).
- [29] R. Shaham, O. Katz, and O. Firstenberg, arXiv e-prints, arXiv:2102.02797 (2021).
- [30] O. Katz, R. Shaham, and O. Firstenberg, Coupling light to a nuclear spin gas with a two-photon linewidth of five millihertz, *Sci. Adv.* **7**, eabe9164 (2021).
- [31] O. Katz, R. Shaham, E. S. Polzik, and O. Firstenberg, Long-Lived Entanglement Generation of Nuclear Spins Using Coherent Light, *Phys. Rev. Lett.* **124**, 043602 (2020), arXiv:2002.07030 [quant-ph].
- [32] O. Katz, R. Shaham, E. Reches, A. V. Gorshkov, and O. Firstenberg, ArXiv arXiv:2007.10177 (2020).
- [33] O. Katz, E. Reches, R. Shaham, A. V. Gorshkov, and O. Firstenberg, ArXiv arXiv:2007.08770v2 (2020).
- [34] T. G. Walker and W. Happer, Spin-exchange optical pumping of noble-gas nuclei, *Rev. Mod. Phys.* **69**, 629 (1997).
- [35] S. Appelt, A. B. Baranga, C. J. Erickson, M. V. Romalis, A. R. Young, and W. Happer, Theory of spin-exchange optical pumping of  $^3\text{He}$  and  $^{129}\text{Xe}$ , *Phys. Rev. A* **58**, 1412 (1998).
- [36] M. V. Romalis, D. Sheng, B. Saam, and T. G. Walker, Comment on “New Limit on Lorentz-Invariance- and CPT-Violating Neutron Spin Interactions Using a Free-Spin-Precession  $^3\text{He}^{129}\text{Xe}$  Comagnetometer”, *Phys. Rev. Lett.* **113**, 188901 (2014).
- [37] D. K. Walter, W. Happer, and T. G. Walker, Estimates of the relative magnitudes of the isotropic and anisotropic magnetic-dipole hyperfine interactions in alkali-metal–noble-gas systems, *Phys. Rev. A* **58**, 3642 (1998).
- [38] S. R. Schaefer, G. D. Cates, T.-R. Chien, D. Gonatas, W. Happer, and T. G. Walker, Frequency shifts of the magnetic-resonance spectrum of mixtures of nuclear spin-polarized noble gases and vapors of spin-polarized alkali-metal atoms, *Phys. Rev. A* **39**, 5613 (1989).
- [39] G. Vasilakis, V. Shah, and M. V. Romalis, Stroboscopic Backaction Evasion in a Dense Alkali-Metal Vapor, *Phys. Rev. Lett.* **106**, 143601 (2011), arXiv:1011.2682 [quant-ph].
- [40] R. Shaham, O. Katz, and O. Firstenberg, Quantum dynamics of collective spin states in a thermal gas, *Phys. Rev. A* **102**, 012822 (2020), arXiv:2006.04243 [quant-ph].
- [41] G. Vasilakis, *Precision Measurements of Spin Interactions with High Density Atomic Vapors* (Princeton University, Princeton, New Jersey, US, 2011).
- [42] C. Gardiner, P. Zoller, and P. Zoller, *Quantum Noise: a Handbook of Markovian and non-Markovian Quantum Stochastic Methods with Applications to Quantum Optics* (Springer Science & Business Media, Berlin, Germany, 2004).
- [43] O. Firstenberg, M. Shuker, A. Ron, and N. Davidson, Colloquium: coherent diffusion of polaritons in atomic media, *Rev. Mod. Phys.* **85**, 941 (2013), arXiv:1207.6748 [quant-ph].
- [44] Z. Wu, S. Schaefer, G. D. Cates, and W. Happer, Coherent interactions of the polarized nuclear spins of gaseous atoms with the container walls, *Phys. Rev. A* **37**, 1161 (1988).
- [45] T. G. Walker and M. S. Larsen, Adv. At. Mol. Opt. Spin-exchange pumped NMR gyros, *Phys.* **65**, 373 (2016), arXiv:1604.03982 [physics.atom-ph].
- [46] M. S. Safronova, D. Budker, D. DeMille, D. F. J. Kimball, A. Derevianko, and C. W. Clark, Search for new physics with atoms and molecules, *Rev. Mod. Phys.* **90**, 025008 (2018), arXiv:1710.01833 [physics.atom-ph].

- [47] J. Lee, A. Almasi, and M. Romalis, Improved Limits on Spin-Mass Interactions, *Phys. Rev. Lett.* **120**, 161801 (2018), [arXiv:1801.02757 \[hep-ex\]](#).
- [48] T. W. Kornack and M. V. Romalis, Dynamics of Two Overlapping Spin Ensembles Interacting by Spin Exchange, *Phys. Rev. Lett.* **89**, 253002 (2002).
- [49] T. W. Kornack, R. K. Ghosh, and M. V. Romalis, Nuclear Spin Gyroscope Based on an Atomic Comagnetometer, *Phys. Rev. Lett.* **95**, 230801 (2005), [arXiv:physics/0505089 \[physics.atom-ph\]](#).
- [50] C. Gerry and P. Knight, *Introductory Quantum Optics* (Cambridge University Press, Cambridge, England, 2004).
- [51] J. Wesenberg and K. Mølmer, Mixed collective states of many spins, *Phys. Rev. A* **65**, 062304 (2002).
- [52] G. Colangelo, F. Martin Ciurana, G. Puentes, M. W. Mitchell, and R. J. Sewell, Entanglement-Enhanced Phase Estimation Without Prior Phase Information, *Phys. Rev. Lett.* **118**, 233603 (2017).
- [53] I. M. Bloch, G. Ronen, R. Shaham, O. Katz, T. Volansky, and O. Katz, for the NASDUCK Collaboration, Nasduck: New constraints on axion-like dark matter from floquet quantum detector (2021), [arXiv:2105.04603 \[hep-ph\]](#).
- [54] M. Jiang, H. Su, A. Garcon, X. Peng, and D. Budker, Search for axion-like dark matter with spin-based amplifiers (2021), [arXiv:2102.01448 \[hep-ph\]](#).
- [55] D. Sheng, S. Li, N. Dural, and M. V. Romalis, Sub-femtotesla Scalar Atomic Magnetometry Using Multipass Cells, *Phys. Rev. Lett.* **110**, 160802 (2013), [arXiv:1208.1099 \[physics.atom-ph\]](#).
- [56] W. C. Chen, T. R. Gentile, Q. Ye, T. G. Walker, and E. Babcock, On the limits of spin-exchange optical pumping of  $^3\text{He}$ , *J. Appl. Phys.* **116**, 014903 (2014).
- [57] I. M. Savukov and M. V. Romalis, Effects of spin-exchange collisions in a high-density alkali-metal vapor in low magnetic fields, *Phys. Rev. A* **71**, 023405 (2005).
- [58] I. K. Kominis, T. W. Kornack, J. C. Allred, and M. V. Romalis, in *APS Division of Atomic, Molecular and Optical Physics Meeting Abstracts*, APS Meeting Abstracts, Vol. 34 (2003), p. G5.002.
- [59] O. Katz, M. Dikopoltsev, O. Peleg, M. Shuker, J. Steinhauer, and N. Katz, Nonlinear Elimination of Spin-Exchange Relaxation of High Magnetic Moments, *Phys. Rev. Lett.* **110**, 263004 (2013), [arXiv:1305.4326 \[quant-ph\]](#).
- [60] M. E. Limes, D. Sheng, and M. V. Romalis,  $^3\text{He}$ - $^{129}\text{Xe}$  Comagnetometry using  $^{87}\text{Rb}$  Detection and Decoupling, *Phys. Rev. Lett.* **120**, 033401 (2018), [arXiv:1708.05772 \[physics.atom-ph\]](#).
- [61] O. Katz and O. Firstenberg, Light storage for one second in room-temperature alkali vapor, *Nat. Commun.* **9**, 2074 (2018).
- [62] K. B. Dideriksen, R. Schmiege, M. Zugenmaier, and E. S. Polzik, [ArXiv arXiv:2010.06875 \[quant-ph\]](#) (2020).
- [63] B. Chann, E. Babcock, L. W. Anderson, T. G. Walker, W. C. Chen, T. B. Smith, A. K. Thompson, and T. R. Gentile, Production of highly polarized  $^3\text{He}$  using spectrally narrowed diode laser array bars, *J. Appl. Phys.* **94**, 6908 (2003).
- [64] D. A. Gangloff, G. Éthier-Majcher, C. Lang, E. V. Denning, J. H. Bodey, D. M. Jackson, E. Clarke, M. Hugues, C. Le Gall, and M. Atatüre, Quantum interface of an electron and a nuclear ensemble, *Science* **364**, 62 (2019), [arXiv:1812.07540 \[quant-ph\]](#).
- [65] S. L. Braunstein and P. van Loock, Quantum information with continuous variables, *Rev. Mod. Phys.* **77**, 513 (2005).
- [66] N. Sangouard, C. Simon, H. de Riedmatten, and N. Gisin, Quantum repeaters based on atomic ensembles and linear optics, Finite-N corrections to vlasov dynamics and the range of pair interactions, *Rev. Mod. Phys.* **83**, 33 (2011).
- [67] A. Gabrielli, M. Joyce, and J. Morand, *Phys. Rev. E* **90**, 062910 (2014), [arXiv:1408.0999 \[cond-mat.stat-mech\]](#).
- [68] J. Pascale, Use of  $l$ -dependent pseudopotentials in the study of alkali-metal-atom—He systems. The adiabatic molecular potentials, *Phys. Rev. A* **28**, 632 (1983).